FERMILAB-Pub-03/409-A

# A Survey of Open Clusters in the $u'g'r'i'z'$ Filter System: I. Results for NGC 2548 (M 48)

Cristin J. Rider[1,2,3,4], Douglas L. Tucker[2,5], J. Allyn Smith[5,6,7,8], Chris Stoughton[2], Sahar S. Allam[2,5,9], Eric H. Neilsen Jr.[2]

## ABSTRACT

We present initial results of a photometric survey of open star clusters, primarily in the southern hemisphere, taken in the $u'g'r'i'z'$ filter system. While our entire observed sample covers more than 100 clusters, here we present data for NGC 2548 (M 48) which is a cluster characterized in the *UBV* and *DDO* photometric systems. We compare our results to the published values from other observers and to the Padova theoretical isochrones and metallicity curves. These observations demonstrate that the $u'g'r'i'z'$ filters can play an important role in determining the metallicity of stars and clusters. We begin this series of papers with a study of NGC 2548 because we have obtained data of this cluster not only with our main program telescope, the CTIO Curtis-Schmidt, but also with the US Naval Observatory (USNO) 1.0 m telescope (the telescope used to define the $u'g'r'i'z'$ system), and the Sloan Digital Sky Survey (SDSS) 0.5 m Photometric Telescope (the photometric monitoring telescope used to calibrate the SDSS 2.5 m telescope imaging data). We have used the data from this study to validate our ability to transform measurements obtained on other telescopes to the standard USNO 1.0 m $u'g'r'i'z'$ system. This validation is particularly important for very red stars, for which the original $u'g'r'i'z'$ standard star network is poorly constrained.

[1]Boston University, Astronomy Department, Boston University, 725 Commonwealth Avenue, Boston, MA 02215

[2]Fermi National Accelerator Laboratory, P.O. Box 500, Batavia, IL 60510

[3]Fermi National Accelerator Laboratory Internship for Undergraduate Physics Majors program.

[4]Current address Johns Hopkins University, Department of Physics & Astronomy, Homewood Campus, 3701 San Martin Drive, Baltimore, MD 21218

[5]Visiting Astronomer, US Naval Observatory, Flagstaff, AZ, 86002

[6]Los Alamos National Laboratory, NIS-4, D448, Los Alamos, NM 87545

[7]University of Wyoming, Department of Physics & Astronomy, P.O. Box 3905, Laramie, WY 82071

[8]Visiting Astronomer, Cerro Tololo Inter-American Observatory. CTIO is operated by AURA, Inc. under contract to the National Science Foundation.

[9]New Mexico State University, Astronomy Department, Box 30001, Dept 4500, 1320 Frenger St., Las Cruces NM 88003

*Subject headings:* Galaxy: open clusters and associations: individual, (NGC 2548) Hertzsprung-Russell diagram, stars: abundances

## 1. Introduction

One of the most powerful tools available in astrophysics for exploring and testing theories of star formation, stellar and galactic evolution, and the chemical enrichment history of the Galaxy is the study of open star clusters. Because of this, open clusters have been the subject of intense studies for the past several decades (e.g., Anthony-Twarog, Twarog, & McClure 1979; Geisler & Smith 1984; Anthony-Twarog, Twarog, & Sheeran 1994; Bruntt et al. 1999; Mathieu 2000; see also Friel 1995 and references therein).

We have embarked on a survey of (mostly) southern hemisphere star clusters using the $u'g'r'i'z'$ filter system. The original motivation of the project was to use these clusters, which span a range of ages and metallicities, to "back calibrate" the Sloan Digital Sky Survey (SDSS) [see Gunn et al. (1998) for a description of the SDSS survey camera and York et al. (2000) for a description of the SDSS]. In addition, these data may now be used to verify the recent age and metallicity models of Girardi et al. (2003) and the prior work of Lenz et al. (1998) and to verify and expand upon the $u'g'r'i'z'$ to $UBVRI$ transformations presented in the standard star paper (Smith et al. 2002).

The initial effort in this survey obtained observations for approximately 105 open clusters and a few (<10) "low-density" globular clusters. This approach was driven, in part, as a result of the availability of the Curtis-Schmidt telescope at the Cerro Tololo Inter-American Observatory (CTIO). This telescope was available as a result of one of us (JAS) being at the University of Michigan as a research fellow. The need to perform the survey observations was a result of the impending closure of this wonderful survey telescope. The wide field of this instrument allowed us to survey several clusters over the course of four observing runs, from 1997–2000.

In this, the first paper of our series, we present our results for NGC 2548, also known as M 48, which is an intermediate age open cluster. We chose this particular cluster because we had observations of it from three telescopes: the CTIO Curtis-Schmidt, which is the main telescope for our open clusters program; the 0.5 m Photometric Telescope, which is used to calibrate the imaging data from the SDSS 2.5 m telescope; and, most importantly, the US Naval Observatory (USNO) 1.0 m telescope at Flagstaff Station, which was used to establish the original $u'g'r'i'z'$ standard star network (Smith et al. 2002). These data, especially from the USNO 1.0 m telescope, have allowed us to tie the CTIO Curtis-Schmidt system more strongly to the basic definition of the $u'g'r'i'z'$ system. As a result the findings from the remainder of our open clusters program will be placed on a firmer foundation.

Although NGC 2548 is bright enough to have been cataloged by Messier, it was once thought to be non-existent due to a sign error in Messier's reported coordinates (Wu et al. 2002). While this cluster has been the subject of several proper motion studies (Ebbighausen 1939; Dias, Lépine, &

Alessi 2001; Wu et al. 2002), chemical composition studies (Wallerstein & Conti 1964; Claria 1985; Gilroy 1989), and dynamical studies (Geyer & Nelles 1985; Bergond, Leon, & Guibert 2001), there have been surprisingly few photometric studies (Pesch 1961; Claria 1985). The only photometric study of this cluster consisting of more than five stars is the $UBV$ photoelectric observations obtained by Pesch (1961), who observed 37 stars and divided them into spectral groups. Further, he estimated the reddening to be $E(B-V) = .04 \pm .05$ and the distance to be 630 pc.

In the following sections we present details of the instrumentation and observations, (§2), data reduction and analysis techniques, (§3), results (§4), and planned future work (§5).

## 2. Instrumentation and Observations

### 2.1. $u'g'r'i'z'$ Filter System

The five filters of the $u'g'r'i'z'$ system have effective wavelengths of 3540Å, 4750Å, 6222Å, 7632Å, and 9049Å, respectively, at 1.2 airmasses.[10] They cover the entire wavelength range of the combined atmosphere+CCD response and their construction is described by Fukugita et al. (1996). The $u'g'r'i'z'$ filters have sharp cutoffs by design. The passbands were selected to exclude the strongest night-sky lines; for example O I ($\lambda$5577) and Hg I ($\lambda$5461). The bulk of the $u'$ band response is blueward of the Balmer discontinuity which, when combined with the $g'$ filter, yields high sensitivity to the magnitude of the Balmer jump but at a cost of lower throughput for the narrower $u'$ filter (compared with Johnson $U$). We note the red side of the $z'$ filter is open ended, and therefore subject to potentially large color terms in the transformation equations, dependent upon the choice of detector.

The $u'g'r'i'z'$ magnitude system is a broadband $AB$ system. In other words, rather than selecting some fiducial spectral type to have null colors (as in the $UBVR_cI_c$ system), $AB$ broadband magnitudes are defined by the following equation:

$$m = -2.5 \log \frac{\int d(\log \nu) f_\nu S_\nu}{\int d(\log \nu) S_\nu} - 48.60, \quad (1)$$

where $f_\nu$ is the energy flux per unit frequency on the atmosphere and $S_\nu$ is the system response. Hence in an $AB$ system, an object with a flat spectral energy distribution would have null colors (Oke & Gunn 1983; Fukugita et al. 1996).

To zeropoint the $u'g'r'i'z'$ system, Smith et al. (2002) used the synthetic $AB$ $u'g'r'i'z'$ magnitudes of the F subdwarf BD+17°4708 as calculated by Fukugita et al. (1996). Initial estimates indicate that the $u'g'r'i'z'$ network is offset from a true $AB$ broadband system by no more than

[10] Note that the $g'$ filter has been determined to have an effective wavelength 20 Å bluer than that originally quoted by Fukugita et al. (1996).

about 5% in $u'$ and $z'$ and by no more than about 3% in $g'r'i'$ (see § 4 below), due to uncertainties in the absolute calibration of the synthetic $u'g'r'i'z'$ magnitudes of BD+17°4708.

The $u'g'r'i'z'$ standard star network is composed of 158 stars distributed primarily along the celestial equator and the northern celestial hemisphere (Smith et al. 2002). As a cautionary note, the primary goals for the SDSS are large scale structure studies using galaxies and QSOs, so the first version of the standard network is limited, for the most part, to stars bluer than about M0 to avoid the strengthening metal bands and flare stars.

## 2.2. Telescopes and Observations

As noted above, we are using data from three separate telescopes in this study of NGC 2548: the USNO 1.0 m telescope at Flagstaff Station in Arizona, the SDSS 0.5 m Photometric Telescope (PT) at Apache Point Observatory in New Mexico, and the University of Michigan's 0.6/0.9 m Curtis-Schmidt telescope at CTIO (CTIO-CS) in Chile. We will describe each instrument in turn. A summary of the system parameters is presented in Table 1. A summary of the observing circumstances for the NGC 2548 field is given in Table 2.

### *2.2.1. USNO 1.0 m*

The USNO 1.0 m telescope is of Ritchey–Chrétien design. The observations for our NGC 2548 program on this telescope were obtained on 2002 November 5 and 6 (UT). All of the observations were direct exposures with a thinned, UV-AR coated, Tektronix TK1024 CCD operating at a gain of 7.43±0.41 electrons per ADU with a readnoise of 6.0 electrons. This CCD is similar to the CCDs used in the main SDSS survey camera and the CCD used by the 0.5-m Photometric Telescope at APO. This is the detector which defines the $u'g'r'i'z'$ standard star network. The camera scale of 0.68 arcsec/pixel for this 1024 × 1024 detector produces a field of view of 11.54 arcmin.

During a typical night at the telescope, we generally observed four to five standard fields at the start of the night to determine the extinction. Following this, we would usually observe two to three target fields, and then would alternate between two to three standard and target fields through the remainder of the night, finishing with a longer run of standards (usually four-five). In general, two or three standard fields were observed several times each night to monitor extinction manually at the telescope and to look for changes in the photometricity of the sky. These values were compared with the "all–sky" extinction values determined later during the reduction process. Additional fields were observed throughout the night, near the meridian and at high airmass, in order to provide a good color spread to solve for instrumental color terms.

#### 2.2.2. *Photometric Telescope*

The SDSS 0.5 m PT is a classic Cassegrain with an additional two corrective lenses. The addition of these two corrective lenses increased the field of view to about 43 arcmin and changed the f-ratio from f/8.0 to f/8.8. The CCD is a SITe 2048 × 2048 device with 24 micron (1.15 arcsec) pixels and a UV-AR coating.

The PT observations for our NGC 2548 program were obtained on 2001 December 2 (UT). On this night, observing began by targetting three standard star fields covering a range of airmasses and colors. Similar sequences of observations occurred at roughly 90 minute intervals through the night, which ended with sequence of observations of four standard star fields, providing data approprate for monitoring the stability of the extinction through the night and generating an all-sky photometric solution for the night.

#### 2.2.3. *CTIO Curtis-Schmidt*

The CTIO-CS is a f/3.5 modified Newtonian focus system with a 0.9 m primary mirror and 0.6 m corrector lens. The CTIO-CS observations for our NGC 2548 program were obtained 2000 March 6 (UT). During this observing session, we used the Tek2k#5 (Tektronix TK2048 CCD) detector with the CTIO set of SDSS $u'g'r'i'z'$ filters. The 2048 × 2048 detector has a scale of 2.3 arcsec/pixel, yielding an effective field of view of 1.3 deg. Readout of the chip was driven by two amplifiers and the CCD system was operated under the Arcon control software (version 3.17) at a gain setting #2. This gain setting yielded effective gain and read noise values as given in Table 1. For the CTIO-CS observations, we followed an observing plan similar to that described for the USNO 1.0 m observations (§2.2.1).

## 3. Data Reduction

We performed reductions using version `v8.0` of the SDSS software pipeline `mtpipe` (see Tucker et al. 2003). This version of `mtpipe` is being used for the current PT reductions used in calibrating the SDSS imaging data (e.g., Abazajian et al. 2003) and in the CTIO-0.9 m reductions used for establishing a southern $u'g'r'i'z'$ standard star network (Smith et al. 2003)[11]. An earlier version of `mtpipe` (`v6.6`) was used for processing the data for the setup of the original $u'g'r'i'z'$ standard star network (Smith et al. 2002). (The main changes between `mtpipe v6.6` and `v8.0` lie in the latter version's increased support for the PT and the CTIO telescopes and its use of an improved set of photometric equations.)

The `mtpipe` pipeline consists of four main packages:

---

[11] `http://home.fnal.gov/~dtucker/Southern_ugriz/index.html`

- `preMtFrames`, which creates the directory structure for the reduction of a night's data, including parameter files needed as input for the other three packages, and runs quality-assurance tests on the raw data.

- `mtFrames`, which processes the images and performs object detection and aperture photometry on target field images. The processing steps include bias (zero) subtraction, flat-field and fringe-frame correction.

- `excal`, which takes the aperture photometry lists for the standard star target fields (i.e., stars from Smith et al. 2002), identifies the individual standard stars within those fields, and fits the observed raw counts and known $u'g'r'i'z'$ magnitudes to a set of photometric equations to obtain extinction and zero point coefficients. The output from this package allows us to monitor the stability of the night. The default analysis block is three hours, but can be changed as required based upon the data present and upon trends in the reductions. Typically, a minimum of ten standard stars are required to obtain a good solution for the night.

- `kali`, which applies the fitted photometric equations to the aperture photometry lists of program target fields for the appropriate analysis block (e.g., the NGC 2548 field).

The photometric equations employed in `excal` for the current paper are the following:

$$\begin{aligned} u'_{\rm inst} &= u'_{\rm o} + a_u + k_u X \\ &+ b_u[(u'-g')_{\rm o} - (u'-g')_{\rm o,zp}] \\ &+ c_u[(u'-g')_{\rm o} - (u'-g')_{\rm o,zp}][X - X_{\rm zp}]\ , \end{aligned} \tag{2}$$

$$\begin{aligned} g'_{\rm inst} &= g'_{\rm o} + a_g + k_g X \\ &+ b_g[(g'-r')_{\rm o} - (g'-r')_{\rm o,zp}] \\ &+ c_g[(g'-r')_{\rm o} - (g'-r')_{\rm o,zp}][X - X_{\rm zp}]\ , \end{aligned} \tag{3}$$

$$\begin{aligned} r'_{\rm inst} &= r'_{\rm o} + a_r + k_r X \\ &+ b_r[(r'-i')_{\rm o} - (r'-i')_{\rm o,zp}] \\ &+ c_r[(r'-i')_{\rm o} - (r'-i')_{\rm o,zp}][X - X_{\rm zp}]\ , \end{aligned} \tag{4}$$

$$\begin{aligned} i'_{\rm inst} &= i'_{\rm o} + a_i + k_i X \\ &+ b_i[(i'-z')_{\rm o} - (i'-z')_{\rm o,zp}] \\ &+ c_i[(i'-z')_{\rm o} - (i'-z')_{\rm o,zp}][X - X_{\rm zp}]\ , \end{aligned} \tag{5}$$

$$\begin{aligned} z'_{\rm inst} &= z'_{\rm o} + a_z + k_z X \\ &+ b_z[(i'-z')_{\rm o} - (i'-z')_{\rm o,zp}] \\ &+ c_z[(i'-z')_{\rm o} - (i'-z')_{\rm o,zp}][X - X_{\rm zp}]. \end{aligned} \tag{6}$$

Taking the $g'$ equation as an example, we note that $g'_{\rm inst}$ is the measured instrumental magnitude, $g'_{\rm o}$ is the extra-atmospheric magnitude, $(g' - r')_{\rm o}$ is the extra-atmospheric color, $a_g$ is the nightly zero point, $k_g$ is the first order extinction coefficient, $b_g$ is the system transform coefficient, $c_g$ is the second order (color) extinction coefficient, and $X$ is the airmass of the observation. The zeropoint constants, $X_{\rm zp}$ and $(g' - r')_{\rm o,zp}$ were defined, respectively, to be the average standard star observation airmass $< X > = 1.3$ and the "cosmic color," as listed in Table 3 of Smith et al. (2002).

In general we follow the reduction procedures outlined in § 3 of Smith et al. (2003), with the following exceptions:

**USNO 1.0 m:** Since this combination of telescope+detector+filters *defines* the $u'g'r'i'z'$ photometric system, we do not solve for the coefficient of the the intrumenal color terms (the "b" terms), but set them all identically to zero. Further, due to variations in seeing during the nights we observed NGC 2548 on this telescope, we found that a larger aperture size yielded stabler aperture photometry and improved residuals in the fits to the photometric equations; so, instead of the 14.86 arcsec aperture diameter used in Smith et al. (2003), we used the 24.0 arcsec aperture diameter originally employed in the setup of the $u'g'r'i'z'$ standard star network (Smith et al. 2002).

**Photometric Telescope:** The data from the PT for this night was originally reduced as part of the standard SDSS photometric calibration program. Currently, as part of this program, `mtFrames` performs aperture photometry using two default aperture sizes: a large aperture of 24.0 arcsec and a small aperture of 12.0 arcsec diameter. The large aperture size is used on the $u'g'r'i'z'$ standard star target fields. The small aperture size is used on the program target fields. A correction to convert the small aperture counts to large aperture counts is calculated for program target fields on an image-by-image basis by measuring the ratio of the fluxes in both apertures for the 12 brightest stars in the image and taking a clipped mean; sanity checks prevent the inclusion of saturated stars, cosmic rays, or close optical doubles in this calculation. The resulting aperture correction is applied to all the stars in the target field.

We took the original `mtFrames` aperture photometry for this night's data and re-ran `excal` and `kali` on it. We did not solve for the $b$ term coefficients but set them to the site-average values for the current PT $u'g'r'i'z'$ filter set (see Table 3 below). Further, rather than solve the photometric equations in 3-hour blocks, we followed the standard SDSS convention used in `mtpipe` processing and used a full-night block.

Note that, in this paper, we follow a slightly different tack in calibrating the PT data than is done for normal SDSS operations. In particular, in normal SDSS operations, different values are used for the zeropoint colors and in the photometric equations the $i'$ filter is indexed to $r' - i'$, not to $i' - z'$ (as in eq. [5] above). We have compared the results from both PT calibration strategies for this night's data, and find typical offsets in the calibrated magnitudes for any given star to be $\ll 0.01$ mag. (For a detailed description of the PT calibration strategy in normal SDSS operations, see Tucker et al. 2003.)

**CTIO Curtis-Schmidt:** To tighten the scatter in the residuals, we chose to fit the photometric equations in `excal` using a single, full-night block instead of multiple 3-hour blocks. Other than that, for this telescope, we follow the data reduction methodology of Smith et al. (2003) very closely.

The night characterization data for each of the photometric nights included in this study of NGC 2548 are given in Table 3. These data include the Modified Julian Date[12] of the observation (col. [1]), filter (col. [2]), zero points (col. [3]), system transformation terms (col. [4]), and first-order extinction terms (col. [5]–[7]). Finally, columns (8) and (9) give the rms errors for, and numbers of, the standard stars observed that night which were used in the photometric solutions. In a footnote, we also list the second-order extinction terms derived in Smith et al. (2002).

Once we had run all the nights containing NGC 2548 data through `mtpipe`, we had ten lists of calibrated NGC 2548 $u'g'r'i'z'$ photometry — one for each targetting of this cluster (see Table 2). In order to compare cross-calibrations, we first combined the contents of these lists by telescope. In other words, we combined the contents of the seven USNO 1.0 m lists together into one large USNO 1.0m list, and we likewise combined the contents of the two CTIO-CS lists into a single large CTIO-CS list.. (Since there was only one PT list to begin with, its contents did not need to be combined.) We did the combining by assigning each star in the combined list the "best" magnitude of its corresponding entries from all $N$ lists for that telescope. In this context, "best" refers to the magnitude that has the smallest photon noise. This is done on a filter-by-filter basis, so a star's best $u'$ magnitude and best $r'$ magnitude may come from different lists. (Star entries were matched by position between lists using a $\pm 2$ arcsec box in RA and DEC.) Magnitude entries which have been flagged by `mtFrames` as being saturated or which have poorly determined values (magnitudes $< 0$ or $> 100$) were excluded from the combine procedure.

To reduce field star contamination only stars within a cluster radius of 27 arcmin (Lyngå 1987) were included in the final telescope lists. Where possible, a cluster membership probability based upon Dias, Lépine, & Alessi (2001)'s proper motion study was assigned to each star.

The full data tables for each telescope are available in the electronic edition of this paper. The available data for each of the telescopes include our internal ID number for each star (col. [1]), the star ID number from Jean-Claude Mermilliod's `webda` online open cluster database[13] (col. [2]), RA (col [3]), DEC (col. [4]), $u'g'r'i'z'$ magnitudes (cols. [5], [6], [7], [8], & [9], respectively), $u'g'r'i'z'$ magnitude (photon noise) errors (cols. [10], [11], [12], [13], & [14], respectively), and $u'g'r'i'z'$ saturation flags (cols. [15], [16], [17], [18], & [19], respectively). Lastly column (20) gives the stars proper motion membership probability from Dias, Lépine, & Alessi (2001). Tables 4, 5, and 6 show the first 50 entries of the available data for the USNO 1.0 m, PT, and CTIO Curtis-Schmidt telescopes, respectively.

We also created a master list in which the lists from all three telescopes were combined. We

---

[12]The Modified Julian Date is defined by the relation MJD≡JD−2,400,000.5, where JD is the Julian Date.

[13]`http://obswww.unige.ch/webda/webda.html`

base our internal numbering scheme (col. [1] of Tables 4, 5, and 6) on this final, master list.

## 4. Results

### 4.1. System Verification

The USNO 1.0 m telescope defines the $u'g'r'i'z'$ filter system. We verify our ability to apply this system to other telescopes by comparing our observations from those telescopes to those from the USNO 1.0 m telescope. This was done by determining the difference in the magnitude, for each filter, for all stars observed by both telescopes. Figures 1 and 2 show, respectively, the differences in magnitude as a function of magnitude and as a function of color between the USNO 1.0 m telescope and the PT. Likewise, Figures 3 and 4 show, respectively, the differences in magnitude as a function of magnitude and as a function of color between the USNO 1.0 m telescope and the CTIO Curtis-Schmidt telescope. As measured by the median magnitude offsets in each filter, there is a $\lesssim$2.2% ($\leq$0.022 mag) systematic difference between the USNO 1.0 m and the PT magnitudes and — except for the $z'$ band — a $\lesssim$2.4% ($\leq$0.024 mag) systematic difference between the USNO 1.0 m and the CTIO Curtis-Schmidt magnitudes. Furthermore, Figures 1, 2, 3 and 4 indicate that there are no strong overall trends in the systematic differences as a function of magnitude or color for these telescopes. The somewhat larger USNO 1.0 m/CTIO-CS $z'$ band offset (0.042 mag or about 4.2%) could be ascribed to just random variations in the atmosphere (note the relatively high rms in the fit to the $z'$ photometric equation for the this night on the CTIO-CS in Table 3). It may also indicate a difficulty in performing $z'$ band aperture photometry with this instrument. This issue will likely be resolved as we analyze more of the CTIO-CS data in detail.

To further illustrate these results, Figures 5 and 6 show the results for each telescope overplotted in a color-magnitude diagram (Figure 5) and in a color-color diagram (Figure 6). The data for the CTIO Curtis-Schmidt, the PT and the USNO 1.0 m telescopes are plotted in red, black, and blue, respectively. These figures demonstrate that the stars observed by each of the three telescopes fall in the same locus and follow the same trends in both the color-magnitude and the color-color diagrams.

These results verify that we can tie observations from other telescopes to the USNO 1.0 m $u'g'r'i'z'$ system with a high degree of accuracy (typically <2–3% systematics).

### 4.2. The Photometric Properties of NGC 2548

We compare our observations of NGC 2548 to theoretical SDSS isochrones and metallicity curves from Girardi et al. (2003) (see also Girardi et al. 2000; Girardi 2001; Girardi et al. 2002). The input physics for these models are based upon a magnetic hydrodynamic equation of state at temperatures $T < 10^7$ and a fully-ionized gas equation of state at higher temperatures; electron screening is incorporated in the reaction rates. The theoretical evolutionary tracks were converted into the SDSS photometric system using the SDSS 2.5 m telescope *ugriz* filter response functions[14] and the no-overshoot ATLAS9 synthetic atmospheres of Castelli, Gratton, & Kurucz (1997). Updated versions of these isochrones for a variety of metallicities are available at: `http://pleiadi.pd.astro.it/~lgirardi/isoc_photsys.00/isoc_sloan/`.

Note that the Girardi et al. (2003) SDSS isochrones were created using the SDSS 2.5 m telescope *ugriz* filter system, which differs slightly from the USNO 1.0 m $u'g'r'i'z'$ filter system (see, for example Abazajian et al. 2003); furthermore, Girardi et al. (2003) assume that the SDSS 2.5 m *ugriz* system is a perfect $AB$ system. In order to compare the isochrones to our data we first had to adjust the isochones for the known deviation of the SDSS 2.5 m telescope from a true $AB$ system. This was done using the following equations (D. Eisenstein, private communication):

$$u(AB, 2.5\ m) = u(2.5\ m) - 0.040\ , \tag{7}$$
$$g(AB, 2.5\ m) = g(2.5\ m) - 0.009\ , \tag{8}$$
$$r(AB, 2.5\ m) = r(2.5\ m)\ , \tag{9}$$
$$i(AB, 2.5\ m) = i(2.5\ m) + 0.017\ , \tag{10}$$
$$z(AB, 2.5\ m) = z(2.5\ m) + 0.035\ . \tag{11}$$

(The values of the $AB$ offsets in these equations are preliminary and future refinement at the $\pm$ 0.01–0.02 mag level are possible.)

Next, the isochrones were converted from the SDSS 2.5 m *ugriz* system into the USNO 1.0 m $u'g'r'i'z'$ system by making use of the following relations (Tucker et al. 2003) :

$$u(2.5\ m) = u'\ , \tag{12}$$
$$g(2.5\ m) = g' + 0.060((g' - r') - 0.53)\ , \tag{13}$$
$$r(2.5\ m) = r' + 0.035((r' - i)' - 0.21)\ , \tag{14}$$
$$i(2.5\ m) = i' + 0.041((r' - i') - 0.21)\ , \tag{15}$$
$$z(2.5\ m) = z' - 0.030((i' - z') - 0.09)\ . \tag{16}$$

The stars were dereddened using a value of $E(B-V) = 0.31$ from the Dias, et al. (2002) open cluster catalog and the following equations from Stoughton et al. (2002):

$$u' = u'_{red} - 5.155 \times E(B-V)\ , \tag{17}$$
$$g' = g'_{red} - 3.793 \times E(B-V)\ , \tag{18}$$
$$i' = i'_{red} - 2.086 \times E(B-V)\ , \tag{19}$$

[14] `http://archive.stsci.edu/sdss/documents/response.dat`

$$r' = r'_{red} - 2.751 \times E(B-V) \ , \quad (20)$$

$$z' = z'_{red} - 1.479 \times E(B-V) \ . \quad (21)$$

The stars were then compared to the results of the Dias, Lépine, & Alessi (2001) proper motion and membership study of this cluster. Stars with membership probabilities greater than 50% were considered to be members; stars with membership probabilities less than 50% were considered non-members. Further, the stars were matched to a list of known red giants and spectroscopic binaries listed in `webda`. This matchup information helped in fitting the isochrones to the data.

Figures 7(a-f) show the full set of color-magnitude diagrams available in the $u'g'r'i'z'$ filter system. The $g'$ vs. $g'-r'$ (Figure 7b) and the $r'$ vs. $g'-r'$ (Figure 7c) color-magnitude diagrams are most similar to the more recognizable $V$ vs. $B-V$ color-magnitude diagrams. (See Table 7 of Smith et al. 2002 for the transformation equations between the $u'g'r'i'z'$ and the Johnson $UBVR_{\rm c}I_{\rm c}$ photometric systems.) All the color-magnitude diagrams have a well defined main sequence and main sequence turn off.

Figures 8(a-c) show the three color-color diagrams of the $u'g'r'i'z'$ filter system. The $u'-g'$ vs. $g'-r'$ (Figure 8a) color-color diagram is most similar to the more common $U-B$ vs. $B-V$ color-color diagram. In the $u'-g'$ vs. $g'-r'$ color-color diagram the main sequence (top line) and the red giant branch (bottom line) are clearly distinguishable; however, in the $g'-r'$ vs. $r'-i'$ (Figure 8b) and $r'-i'$ vs. $i'-z'$ (Figure 8c) color-color diagrams the main sequence and the red giant branch are degenerate.

We initially adopted the Dias, et al. (2002) values for distance, age, and metallicity of NGC 2548 (769 pc, 0.36 Gyr, +0.08, respectively) as the starting point for fitting the theoretical models. We then adjusted these values to find the best fit by eye. This was done by first adjusting the distance to fit the main sequence, and then adjusting the age and metallicity to best fit the main sequence turn off and the red giant branch. Based upon the Girardi et al. (2003) isochones we find that the cluster data are consistent with a distance in the range of 575 pc to 625 pc, an age in the range of 0.37 Gyr to 0.42 Gyr, and a metallicity in the range of $[Z/Z_{\odot}] = -0.1$ to $+0.1$; however, we find that a distance of 700 pc, an age of 0.40 Gyr and a metallicity of $[Z/Z_{\odot}] = 0.0$ best fit our data. We do note that while some of the diagrams indicates a slightly older age (mainly the $u'-g'$ vs. $g'-r'$ color-color diagram), the majority of the diagrams are best fit by the 0.40 Gyr isochrone. The slight discrepancies in the best-fit parameters among these diagrams are within the uncertainties of the isochrones and the $AB$ offsets. Our finding for the metallicity, age, and distance for NGC 2548 are consistent with the Dias, et al. (2002) values. We find an age that is 0.04 Gyr (10%) older and a distance that is 70 pc (10%) closer than the values listed in Dias, et al. (2002). Each of the color-magnitude diagrams and the color-color diagram (Figures 7 and 8) have an over-plotted isochrone with these best fit values. The bold portion of the isochrone represent the region in which the $ugriz$ to $u'g'r'i'z'$ transformations are best characterized. Overall, we find the Girardi et al. (2003) isochrones fit our data in a consistent manner and can be used to extract meaningful cluster information (e.g., age and distance). This holds true even bluewards of region where the $ugriz$ to $u'g'r'i'z'$ transformations are best characterized.

## 5. Summary and Future Work

In this first paper of our series, we show that we can effectively tie $u'g'r'i'z'$ observations from other telescopes to those by the USNO 1.0 m telescope and CCD detector — the configuration which *defined* $u'g'r'i'z'$ photometric system — with a high degree of accuracy (typically <2–3% systematics). This lays a firm foundation for the rest of our open cluster project, which derives data primarily from the CTIO Curtis-Schmidt telescope. Also, we have shown that we can effectively fit isochrones and extract useful cluster information using the $u'g'r'i'z'$ filter system. We used these isochrones to determine the age, distance, and metallicity for NGC 2548. Our metallicity value ($[Z/Z_\odot] = 0.0$) is consistent with the currently accepted value listed in the `webda` online database and in the (Dias, et al. 2002) open cluster catalog, as are our age and and distance values. We find a distance of 700 pc (10% closer than the value reported in Dias, et al. 2002) and an age of 0.40 Gyr (10% older than the Dias, et al. 2002 value.)

Our entire sample of observations consists of more than 100 open clusters. Our immediate goal is to publish a sample of open clusters covering a range of ages and metallicities to help better determine the characteristics of the $u'g'r'i'z'$ filter system. To date, we have built and tested the cluster data matching scripts and adjusted isochrone fits. We will pursue the reduction and analyses of the remaining clusters for which we have data. As the SDSS 2.5 m telescope sweeps across open clusters, we'll incorporate those observations into our survey. Further, as time and conditions permit, the SDSS PT may be used for a survey of northern clusters in much the same way the CTIO Schmidt telescope was used in this current effort. It is relatively small (0.5 m) but has a large field of view, making it an ideal instrument for the initial observations of the larger and brighter clusters. Follow-up work for fainter clusters and cluster members will be pursued at available observatories as time permits.

Repeat observations for some of the clusters will be pursued to expand the investigations to find and analyze variable stars (especially RR-Lyr type stars to improve distance estimates). Deeper exposures for some clusters will be obtained to improve the model fits to the lower main sequence and reduce the scatter that is present in our reconnaissance images.

The authors would like to thank the tremendous support given by the mountain staff at CTIO, especially by Edgardo Cosgrove and Arturo Gomez. We would also like to thank Jeff Pier and Jeff Munn for providing access and support for our observations with the US Naval Observatory 1 m telescope at Flagstaff Station, Arizona, and Alan Uomoto of Johns Hopkins University for providing a working monitor telescope (in the form of the PT) at Apache Point Observatory. We all gratefully acknowledge the support of Leo Girardi for his models and suggestions to improve the fits to the data. We also extend thanks to Daniel Eisenstein, Eva Grebel, Christy Tremonti, and the other members of the SDSS Stars and Calibration Working Groups for suggestions regarding the correct values of the *AB* offsets to use in our isochrone fits. We further acknowledge the `webda` open cluster data compilation which made accessing all available data for this clusters an easy task.

CJR acknowledges support from the Fermi National Accelerator Laboratory Internship for Undergraduate Physics Majors program during the summer of 2002.

JAS acknowledges support from an American Astronomical Society Small Research Grant and the National Science Foundation through grant AST-0097356, which allowed the observations to be obtained. JAS also acknowledges the University of Michigan, Department of Astronomy for access to the Curtis-Schmidt telescope while a research fellow at the University. JAS also acknowledges the proof reading support and English skills of Jeanne Odermann, whose efforts substantially improved the readability of the text.

This research has made use of the NASA Astrophysics Data System and of the Guide Star Catalog 2.2. The Guide Star Catalog was produced at the Space Telescope Science Institute under U.S. Government grant.

Funding for the Sloan Digital Sky Survey (SDSS) has been provided by the Alfred P. Sloan Foundation, the Participating Institutions, the National Aeronautics and Space Administration, the National Science Foundation, the U.S. Department of Energy, the Japanese Monbukagakusho, and the Max Planck Society. The SDSS Web site is `http://www.sdss.org/`.

The SDSS is managed by the Astrophysical Research Consortium (ARC) for the Participating Institutions. The Participating Institutions are The University of Chicago, Fermilab, the Institute for Advanced Study, the Japan Participation Group, The Johns Hopkins University, Los Alamos National Laboratory, the Max-Planck-Institute for Astronomy (MPIA), the Max-Planck-Institute for Astrophysics (MPA), New Mexico State University, University of Pittsburgh, Princeton University, the United States Naval Observatory, and the University of Washington.

## REFERENCES

Abazajian, K. et al, 2003, preprint (astro-ph/0305492)

Anthony-Twarog, B. J., Twarog, B. A., & McClure, R. D. 1979 ApJ, 233, 188

Anthony-Twarog, B. J., Twarog, B. A., & Sheeran, M. 1994 PASP, 106, 486

Bergond, G., Leon, S., & Guibert, J. 2001, A&A, 377, 462

Bruntt, H., Frandsen, S., Kjeldsen, H., & Andersen, M. I. 1999, A&AS, 140, 135

Castelli, F., Gratton, R. G., & Kurucz, R. L. 1997, A&A, 318, 841

Claria, J. J. 1985, A&AS, 59, 195

Dias, W. S., Lépine, J. R. D., & Alessi, B. S. 2001, A&A, 376, 441

Dias, W. S., Alessi, B. S., Moitinho, A., Lépine, J. R. D., & 2002, A&A, 389, 871

Ebbighausen, E. G. 1939, ApJ, 90, 689

Friel, E. D. 1995, ARA&A, 33, 381

Fukugita, M., Ichikawa, T., Gunn, J. E., Doi, M., Shimasaku, K., & Schneider, D. P. 1996, AJ, 111, 1748

Geisler, D. P., & Smith, V. V. 1984, PASP, 96, 871

Geyer, E. H. & Nelles, B. 1985, A&AS, 62, 301

Gilroy, K. K. 1989, ApJ, 347, 835

Girardi, L., Bressan, A., Bertelli, G., & Chiosi, C. 2000 A&AS, 141, 371

Girardi, L., 2001, astro-ph/0108198

Girardi, L., Bressan, A., Bertelli, G., Chiosi, C., Groenwegen, M.A.T., Marigo, P., Salasnich, B., & Weiss, A. 2002 A&A, 391, 195

Girardi, L., et al. 2003, in preparation

Gunn, J. E., Carr, M., Rockosi, C., Sekiguchi, M., et al. 1998, AJ, 116, 3040

Lenz, D. D., Newberg, H. J., Rosner, R., Richards, G. T., & Stoughton, C. 1998, ApJS, 119, 121

Lyngå, G. 1987, Computer Based Catalogue of Open Cluster Data, 5th ed., (Strasbourg: CDS)

Mathieu, R. D. 2000, ASP Conf. Ser. 198: Stellar Clusters and Associations: Convection, Rotation, and Dynamos, 517

Oke, J. B., & Gunn, J. E. 1983, ApJ, 266, 713

Pesch, P. 1961, ApJ, 134, 602

Smith, J. A., Tucker, D. L., Kent, S. et al. 2002, AJ, 123, 2121

Smith, J. A., Tucker, D. L., Allam, S. S. Rodgers, C. T. 2003, AJ, in press

Stoughton, C., Lupton, R. H., Bernardi, M. et al. 2002, AJ, 123, 485 (EDR paper)

Tucker, D.L. et al., in preparation

Wallerstein, G. & Conti, P. 1964, ApJ, 140, 858

Wu, Z. Y., Tian, K. P., Balaguer-Núñez, L., Jordi, C., Zhao, L., & Guibert, J. 2002, A&A, 381, 464

York, D. G., Adelman, J., Anderson, J. E. et al. 2000, AJ, 120, 1579

---

This preprint was prepared with the AAS LaTeX macros v5.0.

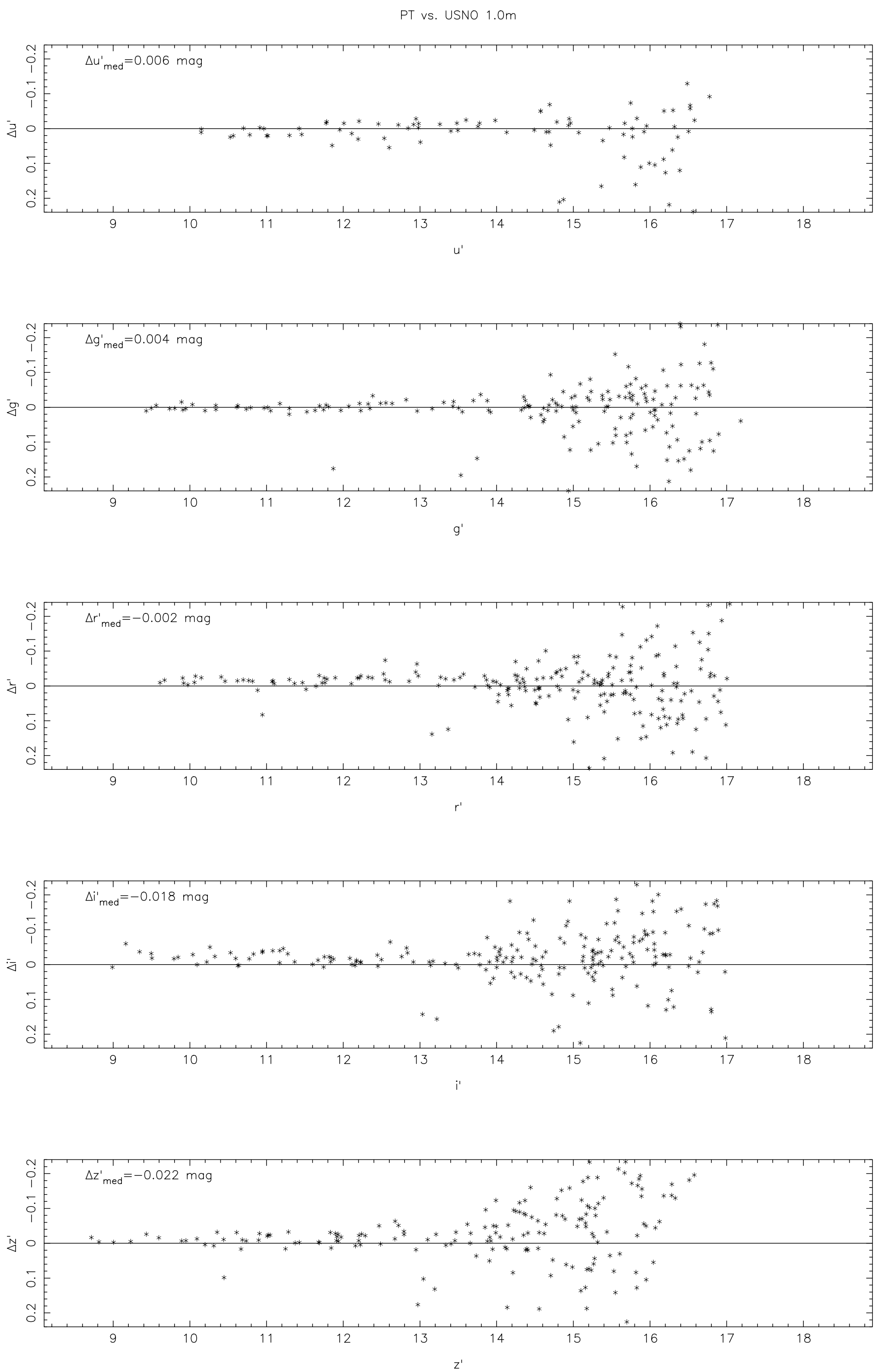


Fig. 1.— Differences between the USNO 1.0 m and the PT magnitudes as a function of apparent magnitude for each of the five filters. The value in the top left corner of each panel is the median magnitude offset between the USNO 1.0 m measurements and the PT measurements in that filter.

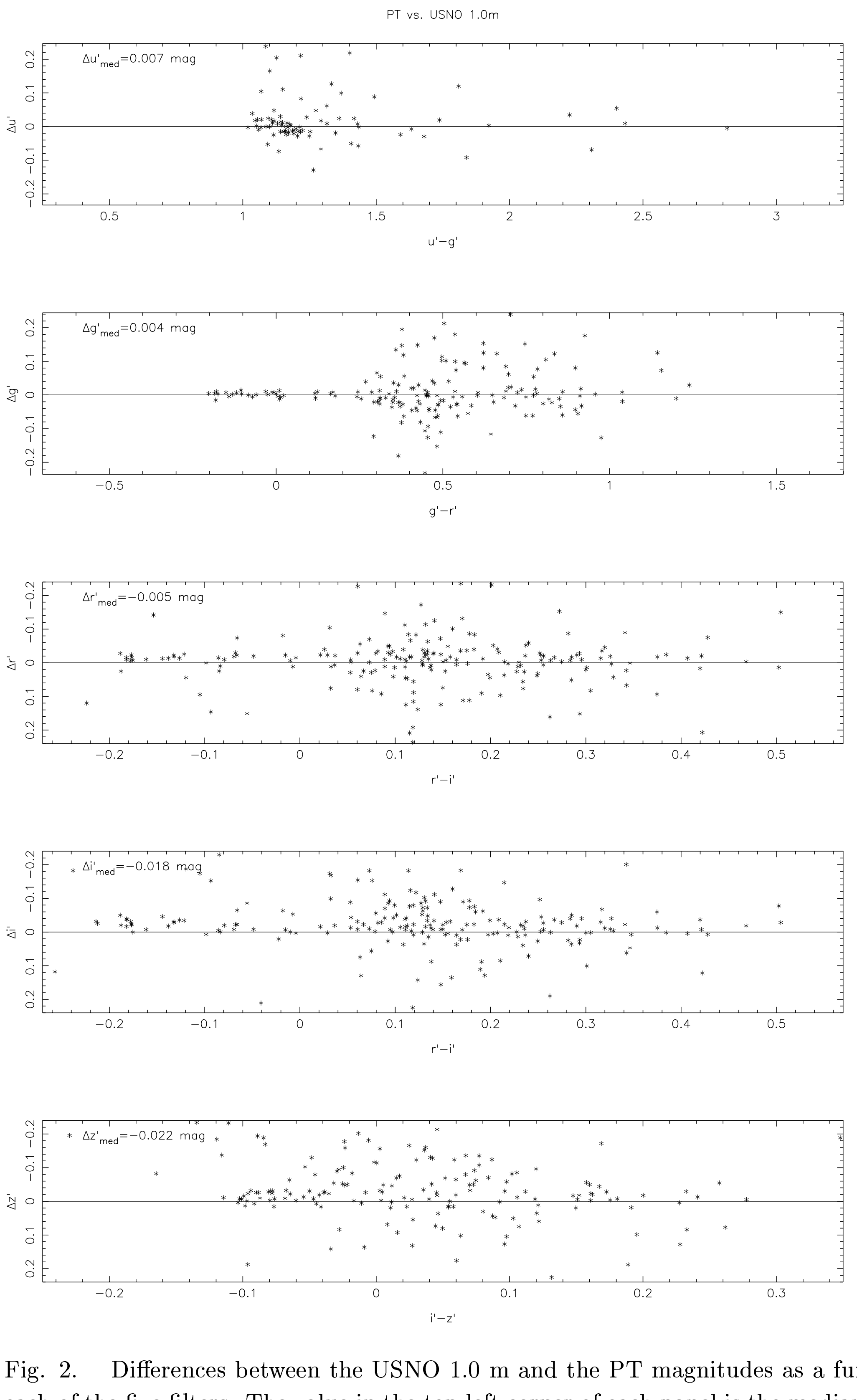


Fig. 2.— Differences between the USNO 1.0 m and the PT magnitudes as a function of color for each of the five filters. The value in the top left corner of each panel is the median magnitude offset between the USNO 1.0 m measurements and the PT measurements in that filter.

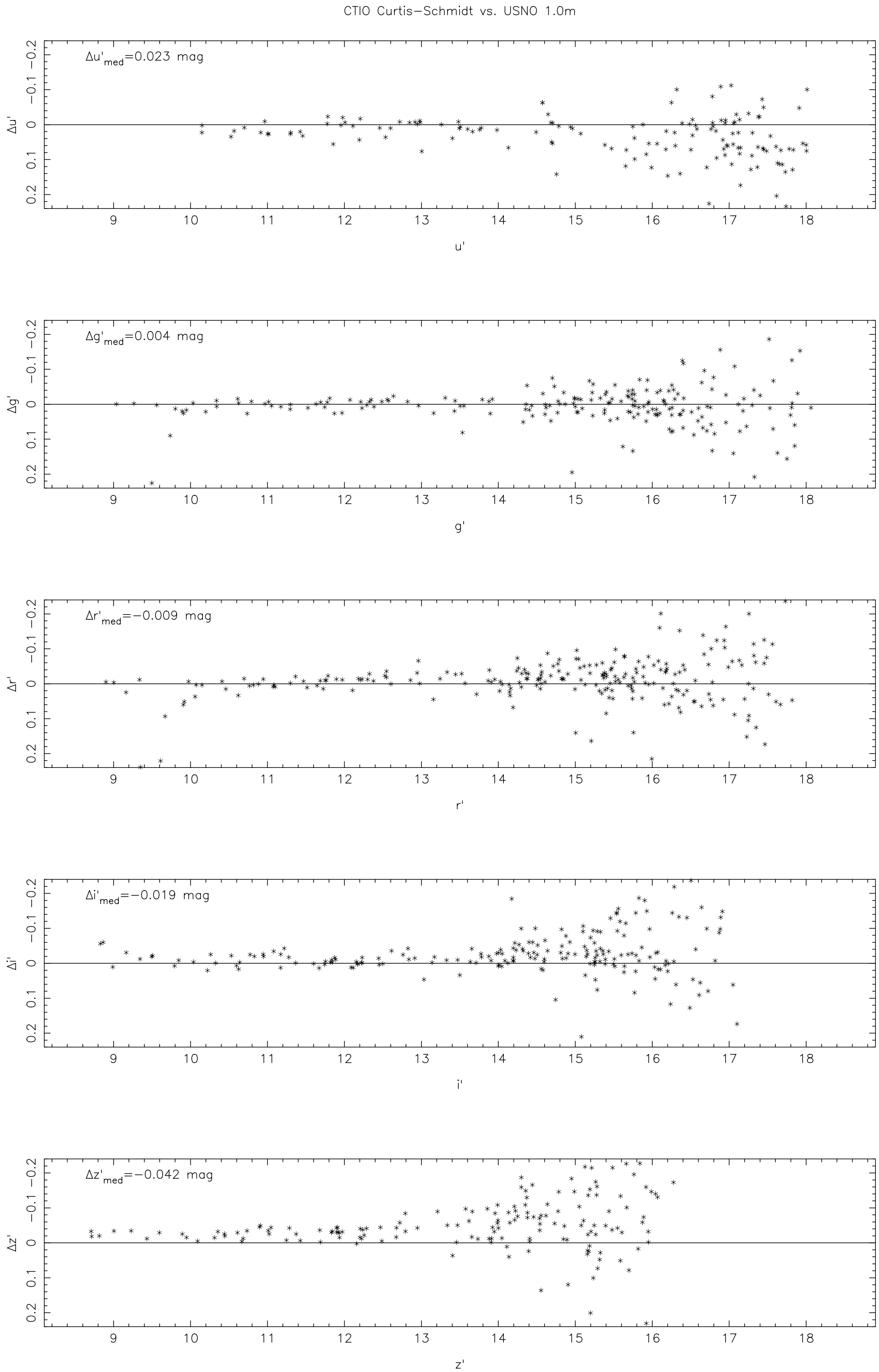


Fig. 3.— Differences between the USNO 1.0 m and the CTIO-CS magnitudes as a function of apparent magnitude for each of the five filters. The value in the top left corner of each panel is the median magnitude offset between the USNO 1.0 m measurements and the CTIO-CS measurements in that filter.

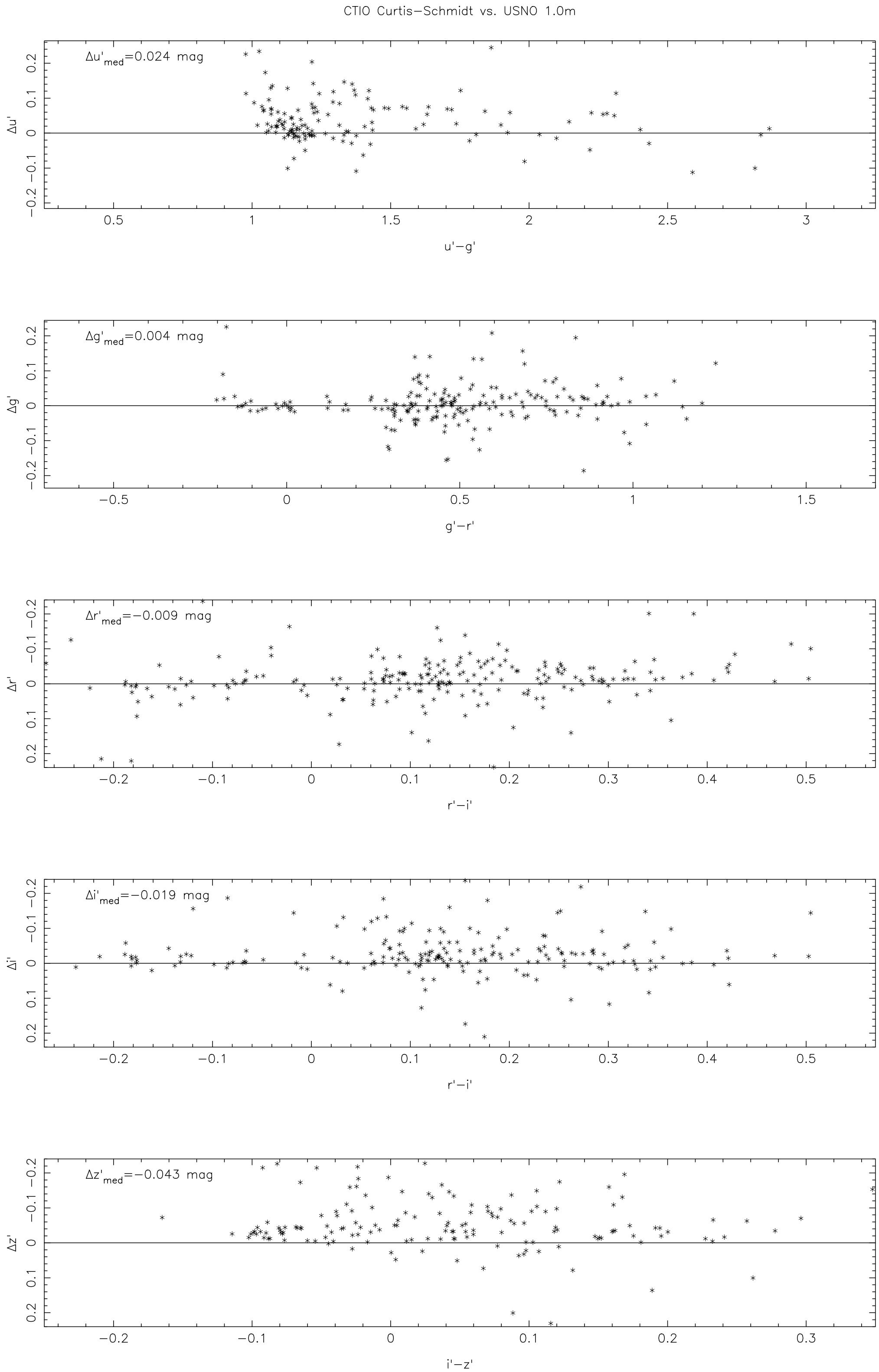


Fig. 4.— Differences between the USNO 1.0 m and the CTIO-CS magnitudes as a function of apparent color for each of the five filters. The value in the top left corner of each panel is the median magnitude offset between the USNO 1.0 m measurements and the CTIO-CS measurements in that filter.

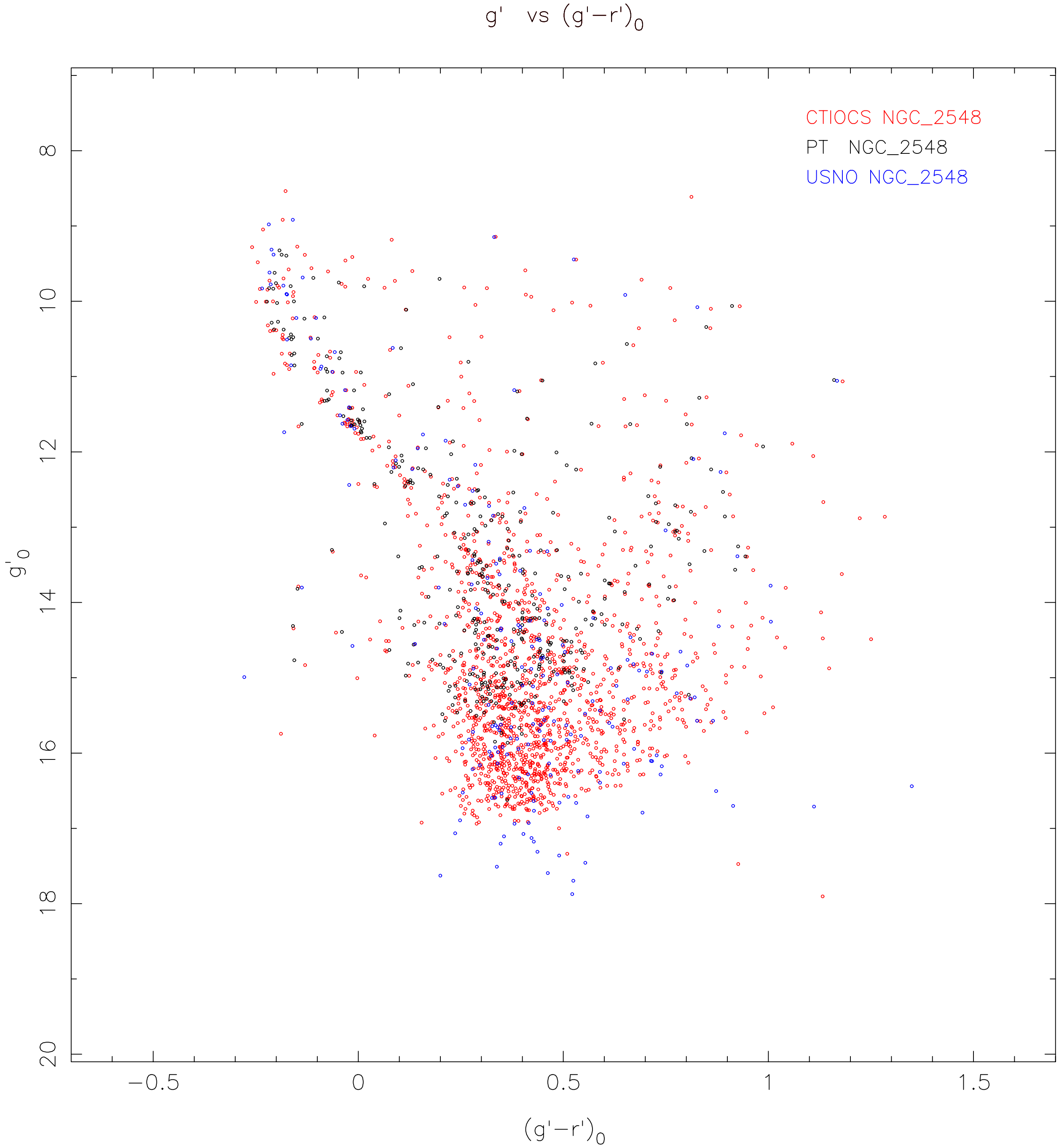


Fig. 5.— A comparison of the de-reddened $g'$ vs. $g' - r'$ color-magnitude diagrams for NGC 2548 obtained from the CTIO-CS (red dots), the PT (black dots), and the USNO 1.0m (blue dots).

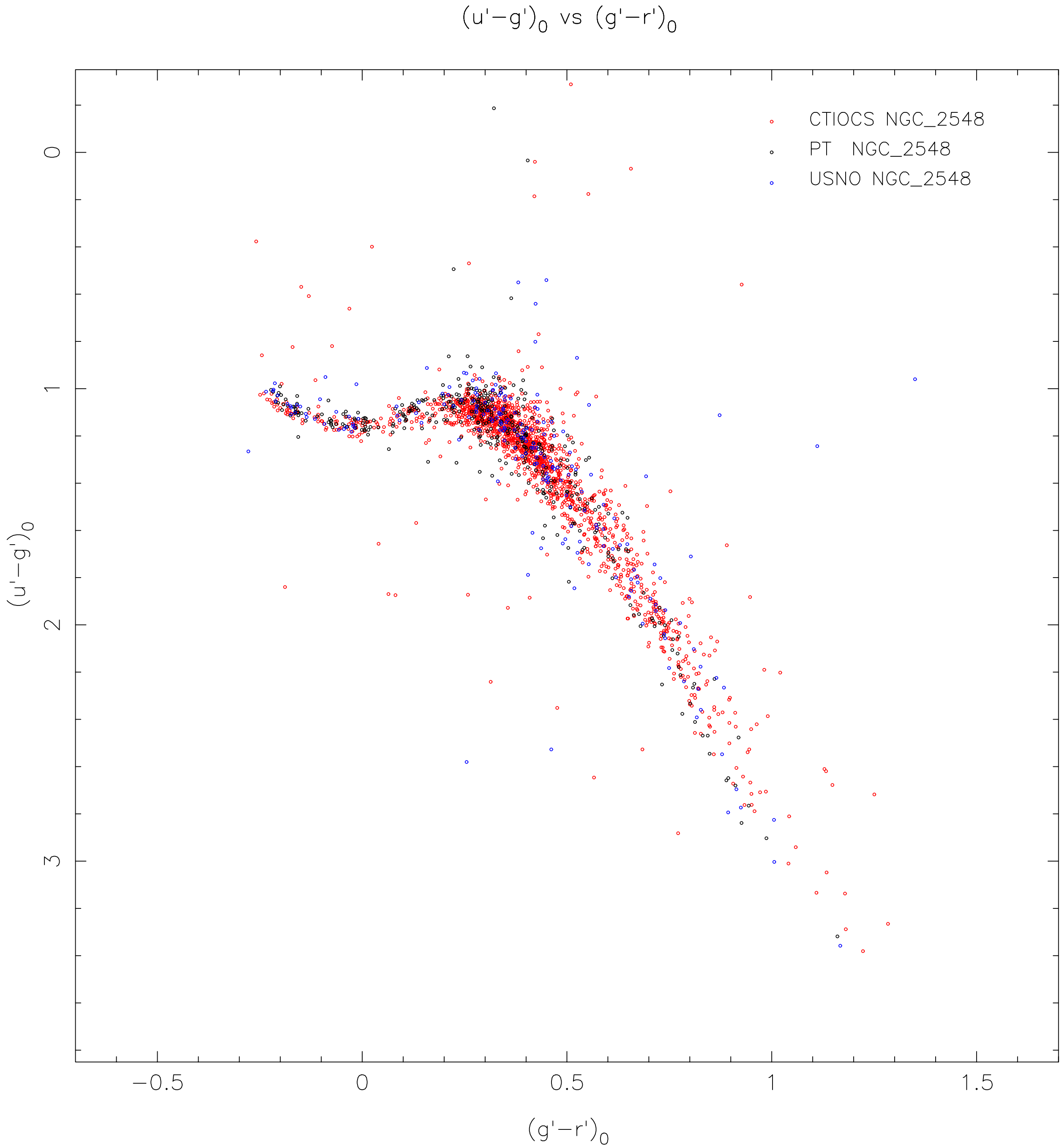


Fig. 6.— A comparison of the de-reddened $u' - g'$ vs. $g' - r'$ color-color diagrams for NGC 2548 obtained from the CTIO-CS (red dots), the PT (black dots), and the USNO 1.0m (blue dots).

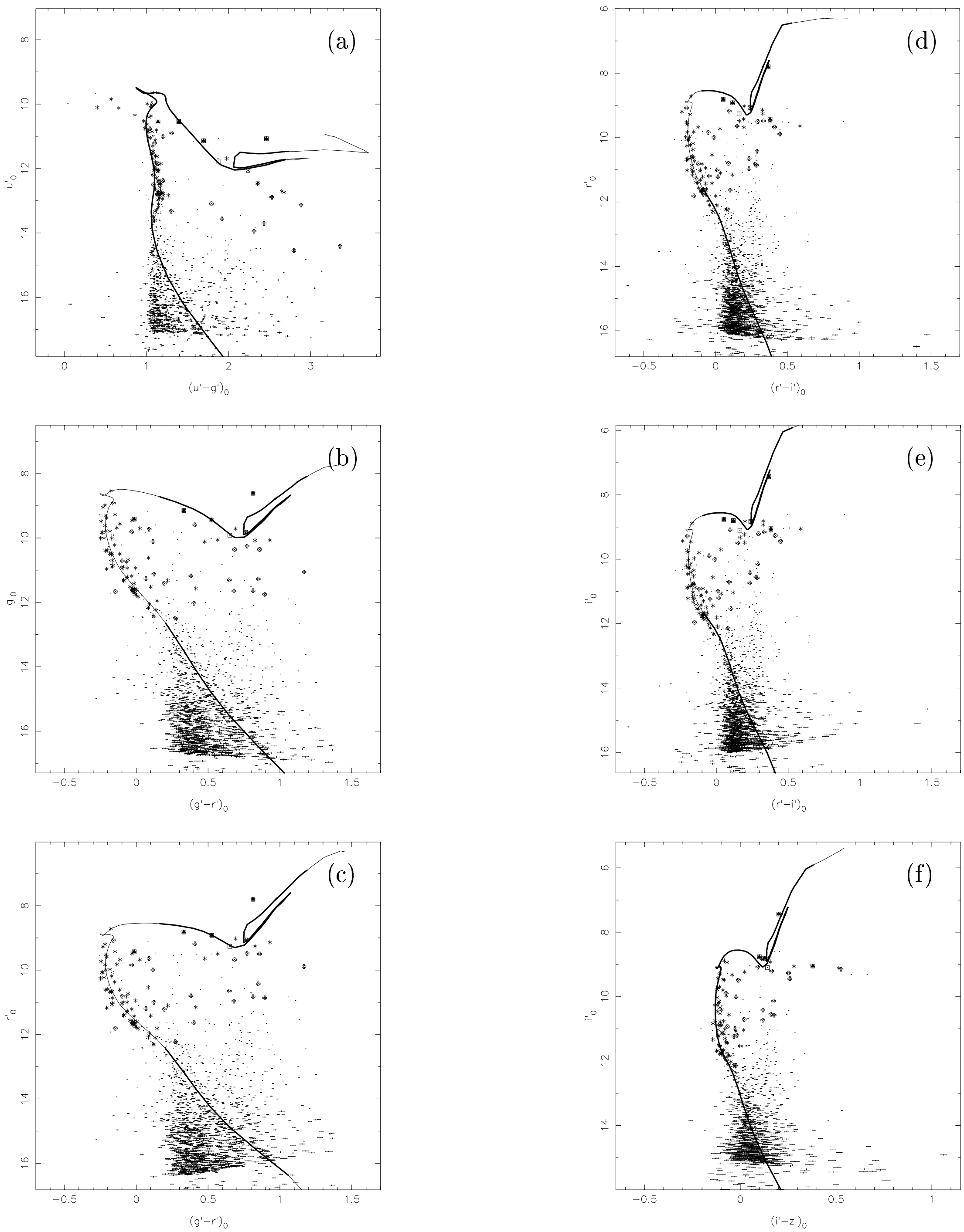


Fig. 7.— The de-reddened color-magnitude diagrams for NGC 2548 using the combined data from all three telescopes. The solid line is the 0.40 Gyr and $[Z/Z_{\odot}] = 0.0$ isochrone from Girardi (2001). Stars judged to be proper motion members, proper motion non-members, red giants, and spectroscopic binaries are plotted as asterisks, crosses, boxes and triangles, respectively.

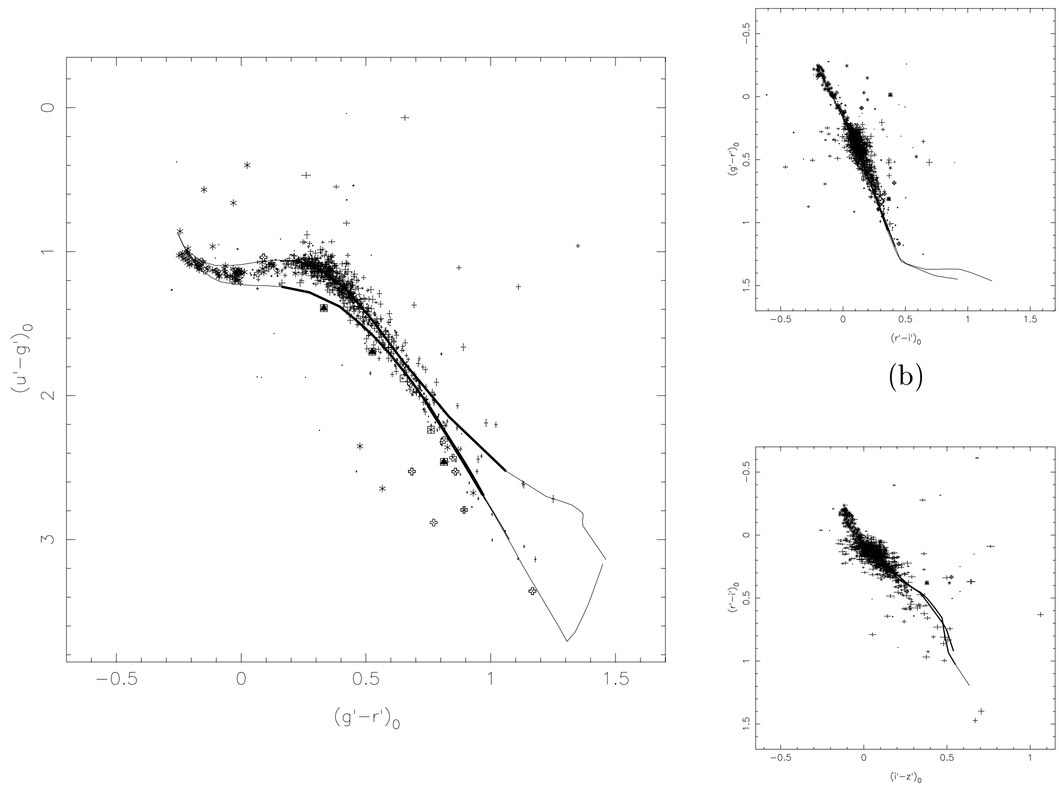


Fig. 8.— The de-reddened color-color diagrams for NGC 2548 using the combined data from all three telescopes. To reduce contamination from field stars, only stars with estimated photon noise errors in the colors less than 0.05 mag are included (typically stars fainter than $g' \approx 15$). The solid line is the 0.40 Gyr and $[Z/Z_{\odot}] = 0.0$ isochrone from Girardi (2001). Stars judged to be proper motion members, proper motion non-members, red giants, and spectroscopic binaries are plotted as asterisks, crosses, boxes and triangles, respectively.

Table 1. Telescope Parameters.

| Telescope | Aperture | Focal Length | Chip | # of Amplifiers | Gain (epadu) | Read Noise ($e^-$) |
|---|---|---|---|---|---|---|
| USNO | 1.0 m | f/7.3 | TK1024 | 1 | 7.43±.41 | 6.0 |
| PT* | 0.5 m | f/8.8 | SITe 2048x2048 | 2 | 4.89±.03, 4.44±0.02 | 7.43 , 7.86 |
| CTIO-CS | 0.6/0.9 m | f/3.5 | TeK2K#5 | 2 | 2.89 (left) 2.90 (right) | 4.1 (left) 4.3 (right) |

*measurements of PT gain and readnoise from Fukugita, M., Ichikawa, S., Watanabe, M., & Yasuda, N., 2000, "Verification of the SDSS Photometric Telecope: I. Electronics," (unpublished SDSS internal document).

Table 2. Observing Circumstances

| YYMMDD | MJD | Airmass | Exposure (sec) | | | | | Comments |
|---|---|---|---|---|---|---|---|---|
| | | | $r'$ | $g'$ | $u'$ | $i'$ | $z'$ | |
| | | USNO 1.0 m | | | | | | |
| 021105 | 52583 | 1.425 | 10 | 10 | 60 | 10 | 15 | Photometric |
| | | 1.408 | 60 | 60 | 360 | 60 | 90 | Photometric |
| | | 1.349 | 10 | 10 | 60 | 10 | 15 | Photometric |
| | | 1.341 | 60 | 60 | 360 | 60 | 90 | Photometric |
| 021106 | 52584 | 1.430 | 10 | 10 | 60 | 10 | 15 | Photometric |
| | | 1.405 | 60 | 60 | 360 | 60 | 90 | Photometric |
| | | 1.369 | 5 | 5 | 30 | 5 | 8 | Photometric |
| | | Photometric Telescope | | | | | | |
| 011202 | 52245 | 1.339 | 15 | 15 | 90 | 15 | 30 | Photometric |
| | | CTIO Curtis-Schmidt | | | | | | |
| 000306 | 51609 | 1.125 | 5 | 5 | 30 | 5 | 5 | Photometric |
| | | 1.137 | 30 | 30 | 240 | 30 | 30 | Photometric |

Table 3. Night Characterization Coefficients[a]

| MJD | Filter | Zeropoint (a) | Instr. Color (b) | 1st-Order Ext. (k) block 0 | block 1 | block 2 | Std. rms (mag) | # Std. stars |
|---|---|---|---|---|---|---|---|---|
| (1) | (2) | (3) | (4) | (5) | (6) | (7) | (8) | (9) |
| | | | | USNO 1.0 m[b] | | | | |
| | | | | 01:47-04:47UT | 04:47-07:47UT | 07:47-12:43UT | | |
| 52583 | $u'$ | -20.036±0.062 | 0.000 | 0.434±0.050 | 0.459±0.041 | 0.432±0.037 | 0.044 | 19 |
| 52583 | $g'$ | -21.654±0.014 | 0.000 | 0.155±0.011 | 0.150±0.010 | 0.147±0.008 | 0.011 | 20 |
| 52583 | $r'$ | -21.517±0.010 | 0.000 | 0.094±0.008 | 0.091±0.007 | 0.086±0.006 | 0.007 | 19 |
| 52583 | $i'$ | -21.079±0.012 | 0.000 | 0.039±0.009 | 0.035±0.008 | 0.033±0.007 | 0.008 | 19 |
| 52583 | $z'$ | -19.974±0.020 | 0.000 | 0.057±0.016 | 0.033±0.013 | 0.029±0.011 | 0.014 | 20 |
| | | | | 01:29-04:29UT | 04:29-07:29UT | 07:29-13:10UT | | |
| 52584 | $u'$ | -20.200±0.044 | 0.000 | 0.556±0.033 | 0.552±0.030 | 0.550±0.032 | 0.039 | 18 |
| 52584 | $g'$ | -21.686±0.021 | 0.000 | 0.180±0.016 | 0.178±0.014 | 0.179±0.016 | 0.019 | 18 |
| 52584 | $r'$ | -21.499±0.012 | 0.000 | 0.088±0.009 | 0.087±0.008 | 0.078±0.009 | 0.010 | 17 |
| 52584 | $i'$ | -21.068±0.013 | 0.000 | 0.043±0.010 | 0.041±0.009 | 0.036±0.010 | 0.012 | 17 |
| 52584 | $z'$ | -19.943±0.020 | 0.000 | 0.049±0.015 | 0.04±10.013 | 0.026±0.015 | 0.018 | 18 |
| | | | | Photometric Telescope[c] | | | | |
| | | | | 02:20-11:12UT | | | | |
| 52245 | $u'$ | -18.959±0.030 | 0.001 | 0.476±0.020 | ··· | ··· | 0.034 | 31 |
| 52245 | $g'$ | -20.776±0.011 | -0.041 | 0.137±0.007 | ··· | ··· | 0.012 | 32 |
| 52245 | $r'$ | -20.686±0.008 | 0.009 | 0.088±0.005 | ··· | ··· | 0.009 | 33 |
| 52245 | $i'$ | -20.215±0.011 | 0.010 | 0.043±0.008 | ··· | ··· | 0.013 | 34 |
| 52245 | $z'$ | -19.266±0.014 | 0.002 | 0.048±0.009 | ··· | ··· | 0.016 | 34 |
| | | | | CTIO Curtis-Schmidt | | | | |
| | | | | 00:27-09:36UT | ··· | ··· | | |
| 51609 | $u'$ | -18.876±0.023 | -0.020±0.008 | 0.516±0.014 | ··· | ··· | 0.020 | 23 |
| 51609 | $g'$ | -20.864±0.012 | 0.013±0.007 | 0.203±0.007 | ··· | ··· | 0.010 | 23 |
| 51609 | $r'$ | -20.794±0.023 | 0.000±0.032 | 0.116±0.014 | ··· | ··· | 0.019 | 23 |
| 51609 | $i'$ | -20.364±0.027 | -0.025±0.049 | 0.077±0.015 | ··· | ··· | 0.022 | 24 |
| 51609 | $z'$ | -19.387±0.017 | 0.029±0.061 | 0.004±0.001 | ··· | ··· | 0.026 | 23 |

[a]The values for the second order extinction term ($c$) coefficients were set to $-2.1 \times 10^{-2}$, $-1.6 \times 10^{-2}$, $-4.0 \times 10^{-3}$, $6.0 \times 10^{-3}$ and $3.0 \times 10^{-3}$, for the $u'$,$g'$,$r'$,$i'$ and $z'$ respectively. These values are those determined in Smith et al. (2002).

[b]The USNO 1.0 m telescope, its Tektronix TK1024 CCD, and its $u'g'r'i'z'$ filter set *define* the $u'g'r'i'z'$ photometric system; hence, the instrumental color term ($b$) values are set to zero by definition.

[c]We have set the instrumental color term ($b$) coefficients for the PT to their site averages rather than solving for them based upon a single night's data.

Table 4. Example of Available Data for the USNO 1.0 m Telescope

| Star ID | WEBDA ID | RA | DEC | Magnitude | | | | | Magnitude Error | | | | | Saturation Flag | | | | | Men Pro |
|---|---|---|---|---|---|---|---|---|---|---|---|---|---|---|---|---|---|---|---|
| | | | | $u'$ | $g'$ | $r'$ | $i'$ | $z'$ | $u'$ | $g'$ | $r'$ | $i'$ | $z'$ | $u'$ | $g'$ | $r'$ | $i'$ | $z'$ | |
| 1 | 2 | 3 | 4 | 5 | 6 | 7 | 8 | 9 | 10 | 11 | 12 | 13 | 14 | 15 | 16 | 17 | 18 | 19 | |
| 3 | 1260 | +08:13:40.3 | -05:46:25 | 10.533 | 9.142 | 8.813 | 8.762 | 8.656 | 0.000 | 0.000 | 0.000 | 0.000 | 0.001 | 0 | 0 | 0 | 0 | 0 | 97 |
| 4 | 1296 | +08:13:44.7 | -05:48:01 | 11.132 | 9.439 | 8.916 | 8.799 | 8.663 | 0.001 | 0.001 | 0.000 | 0.000 | 0.001 | 0 | 0 | 0 | 0 | 0 | 96 |
| 7 | 1313 | +08:13:46.6 | -05:44:52 | 9.981 | 8.913 | 9.075 | 9.279 | 9.379 | 0.000 | 0.000 | 0.000 | 0.000 | 0.000 | 0 | 0 | 0 | 0 | 0 | 5 |
| 11 | 1289 | +08:13:44.1 | -05:48:49 | 9.982 | 8.975 | 9.195 | 9.431 | 9.535 | 0.001 | 0.000 | 0.000 | 0.000 | 0.001 | 0 | 0 | 0 | 0 | 0 | 93 |
| 12 | 870 | +08:12:51.2 | -05:50:51 | 12.433 | 10.074 | 9.250 | 8.925 | 8.761 | 0.001 | 0.001 | 0.001 | 0.001 | 0.001 | 0 | 0 | 0 | 0 | 0 | 87 |
| 13 | 1218 | +08:13:35.3 | -05:53:02 | 11.789 | 9.910 | 9.262 | 9.100 | 8.951 | 0.001 | 0.001 | 0.001 | 0.001 | 0.001 | 0 | 0 | 0 | 0 | 0 | -1 |
| 25 | 978 | +08:13:05.3 | -05:45:01 | 10.361 | 9.309 | 9.523 | 9.727 | 9.839 | 0.000 | 0.001 | 0.001 | 0.000 | 0.000 | 0 | 0 | 0 | 0 | 0 | 96 |
| 28 | 1169 | +08:13:28.6 | -05:48:15 | 10.401 | 9.373 | 9.582 | 9.781 | 9.894 | 0.000 | 0.001 | 0.001 | 0.000 | 0.000 | 0 | 0 | 0 | 0 | 0 | 96 |
| 37 | 1253 | +08:13:39.5 | -05:47:15 | 10.799 | 9.680 | 9.810 | 9.973 | 10.039 | 0.000 | 0.001 | 0.001 | 0.000 | 0.001 | 0 | 0 | 0 | 0 | 0 | 95 |
| 39 | 1117 | +08:13:23.1 | -05:45:23 | 10.616 | 9.612 | 9.831 | 10.029 | 10.144 | 0.000 | 0.001 | 0.001 | 0.000 | 0.001 | 0 | 0 | 0 | 0 | 0 | 97 |
| 41 | 1434 | +08:13:59.6 | -05:53:22 | 14.413 | 11.051 | 9.886 | 9.440 | 9.168 | 0.003 | 0.000 | 0.001 | 0.000 | 0.001 | 0 | 0 | 0 | 0 | 0 | 41 |
| 44 | 975 | +08:13:04.9 | -05:53:05 | 10.851 | 9.787 | 9.972 | 10.156 | 10.258 | 0.000 | 0.001 | 0.001 | 0.000 | 0.001 | 0 | 0 | 0 | 0 | 0 | 89 |
| 45 | 1338 | +08:13:48.9 | -05:44:23 | 10.746 | 9.775 | 9.977 | 10.197 | 10.302 | 0.000 | 0.001 | 0.001 | 0.000 | 0.001 | 0 | 0 | 0 | 0 | 0 | 96 |
| 49 | -1 | +08:13:05.1 | -05:45:11 | -100.000 | -100.000 | 10.051 | 10.339 | -100.000 | -100.000 | -100.000 | 0.001 | 0.001 | -100.000 | 1 | 1 | 0 | 0 | 1 | -1 |
| 50 | 1147 | +08:13:26.5 | -05:49:54 | 10.836 | 9.824 | 10.053 | 10.261 | 10.386 | 0.000 | 0.001 | 0.001 | 0.000 | 0.001 | 0 | 0 | 0 | 0 | 0 | 95 |
| 51 | -1 | +08:13:43.1 | -05:45:53 | 10.970 | 9.897 | 10.075 | 10.295 | 10.394 | 0.000 | 0.000 | 0.000 | 0.000 | 0.001 | 0 | 0 | 0 | 0 | 0 | -1 |
| 53 | -1 | +08:13:42.9 | -05:46:00 | 10.983 | 9.904 | 10.081 | 10.320 | 10.413 | 0.000 | 0.000 | 0.000 | 0.000 | 0.001 | 0 | 0 | 0 | 0 | 0 | -1 |
| 61 | 1306 | +08:13:45.9 | -05:46:02 | 11.260 | 10.222 | 10.313 | 10.465 | 10.557 | 0.001 | 0.001 | 0.001 | 0.000 | 0.001 | 0 | 0 | 0 | 0 | 0 | -1 |
| 62 | 1029 | +08:13:12.1 | -05:46:42 | 11.292 | 10.217 | 10.371 | 10.532 | 10.630 | 0.001 | 0.000 | 0.000 | 0.000 | 0.001 | 0 | 0 | 0 | 0 | 0 | 96 |
| 65 | 848 | +08:12:48.5 | -05:53:45 | 11.688 | 10.614 | 10.533 | 10.560 | 10.612 | 0.001 | 0.000 | 0.000 | 0.000 | 0.001 | 0 | 0 | 0 | 0 | 0 | 52 |
| 71 | 1362 | +08:13:52.0 | -05:54:20 | 11.623 | 10.491 | 10.609 | 10.763 | 10.838 | 0.001 | 0.000 | 0.000 | 0.001 | 0.001 | 0 | 0 | 0 | 0 | 0 | 91 |
| 77 | 1406 | +08:13:57.2 | -05:48:14 | 11.615 | 10.504 | 10.680 | 10.884 | 10.986 | 0.001 | 0.000 | 0.000 | 0.001 | 0.001 | 0 | 0 | 0 | 0 | 0 | 94 |
| 79 | 1424 | +08:13:58.9 | -05:50:40 | 11.848 | 10.670 | 10.730 | 10.878 | 10.962 | 0.001 | 0.000 | 0.000 | 0.001 | 0.001 | 0 | 0 | 0 | 0 | 0 | 96 |
| 81 | 1454 | +08:14:02.9 | -05:50:26 | 12.374 | 11.173 | 10.796 | 10.708 | 10.680 | 0.001 | 0.000 | 0.000 | 0.001 | 0.001 | 0 | 0 | 0 | 0 | 0 | 0 |
| 86 | 1230 | +08:13:36.6 | -05:51:22 | 14.546 | 11.748 | 10.857 | 10.575 | 10.391 | 0.003 | 0.001 | 0.000 | 0.000 | 0.001 | 0 | 0 | 0 | 0 | 0 | 57 |
| 91 | -1 | +08:13:38.7 | -05:47:17 | 11.813 | 10.863 | 10.955 | 10.993 | 11.191 | 0.001 | 0.000 | 0.000 | 0.001 | 0.001 | 0 | 0 | 0 | 0 | 0 | -1 |
| 93 | -1 | +08:13:40.9 | -05:46:56 | 12.044 | 10.892 | 10.986 | 11.153 | 11.226 | 0.001 | 0.000 | 0.000 | 0.001 | 0.001 | 0 | 0 | 0 | 0 | 0 | 87 |
| 95 | 924 | +08:12:58.4 | -05:51:06 | 12.029 | 10.931 | 10.997 | 11.105 | 11.192 | 0.001 | 0.000 | 0.000 | 0.001 | 0.001 | 0 | 0 | 0 | 0 | 0 | 95 |
| 98 | 1268 | +08:13:41.3 | -05:50:55 | 11.949 | 10.845 | 11.011 | 11.211 | 11.314 | 0.001 | 0.000 | 0.000 | 0.001 | 0.001 | 0 | 0 | 0 | 0 | 0 | 96 |
| 108 | 1124 | +08:13:23.6 | -05:50:06 | 12.296 | 11.175 | 11.210 | 11.301 | 11.367 | 0.001 | 0.000 | 0.001 | 0.001 | 0.001 | 0 | 0 | 0 | 0 | 0 | 97 |
| 111 | 1339 | +08:13:49.0 | -05:46:25 | 14.485 | 12.097 | 11.276 | 11.015 | 10.848 | 0.003 | 0.001 | 0.001 | 0.001 | 0.001 | 0 | 0 | 0 | 0 | 0 | -1 |
| 114 | 2529 | +08:13:35.9 | -05:48:34 | 14.530 | 12.268 | 11.381 | 11.107 | 10.951 | 0.003 | 0.001 | 0.001 | 0.001 | 0.001 | 0 | 0 | 0 | 0 | 0 | -1 |
| 118 | 1204 | +08:13:33.4 | -05:53:35 | 12.556 | 11.403 | 11.428 | 11.534 | 11.619 | 0.001 | 0.001 | 0.001 | 0.001 | 0.001 | 0 | 0 | 0 | 0 | 0 | -1 |
| 124 | 1393 | +08:13:55.7 | -05:51:27 | 12.685 | 11.510 | 11.557 | 11.679 | 11.782 | 0.001 | 0.001 | 0.001 | 0.001 | 0.001 | 0 | 0 | 0 | 0 | 0 | 96 |
| 126 | 1364 | +08:13:52.5 | -05:44:24 | 12.756 | 11.570 | 11.592 | 11.689 | 11.772 | 0.001 | 0.001 | 0.001 | 0.001 | 0.001 | 0 | 0 | 0 | 0 | 0 | 97 |
| 129 | -1 | +08:13:23.9 | -05:45:13 | 12.677 | 11.766 | 11.611 | 11.482 | 11.593 | 0.001 | 0.001 | 0.001 | 0.001 | 0.001 | 0 | 0 | 0 | 0 | 0 | -1 |
| 133 | 901 | +08:12:55.4 | -05:45:02 | 12.840 | 11.847 | 11.637 | 11.606 | 11.634 | 0.001 | 0.001 | 0.001 | 0.001 | 0.001 | 0 | 0 | 0 | 0 | 0 | -1 |
| 136 | 1392 | +08:13:55.7 | -05:48:17 | 12.788 | 11.621 | 11.656 | 11.752 | 11.837 | 0.001 | 0.001 | 0.001 | 0.001 | 0.001 | 0 | 0 | 0 | 0 | 0 | -1 |
| 141 | 1324 | +08:13:47.6 | -05:46:00 | 12.822 | 11.654 | 11.675 | 11.777 | 11.872 | 0.001 | 0.001 | 0.001 | 0.001 | 0.001 | 0 | 0 | 0 | 0 | 0 | 96 |
| 143 | 1261 | +08:13:40.2 | -05:54:18 | 12.818 | 11.687 | 11.692 | 11.770 | 11.852 | 0.001 | 0.001 | 0.001 | 0.001 | 0.001 | 0 | 0 | 0 | 0 | 0 | 97 |
| 151 | 1438 | +08:14:00.3 | -05:49:57 | 13.098 | 11.956 | 11.801 | 11.809 | 11.857 | 0.001 | 0.001 | 0.001 | 0.001 | 0.001 | 0 | 0 | 0 | 0 | 0 | 88 |
| 158 | 2531 | +08:13:53.1 | -05:49:21 | 13.345 | 12.174 | 11.878 | 11.820 | 11.840 | 0.001 | 0.001 | 0.001 | 0.001 | 0.001 | 0 | 0 | 0 | 0 | 0 | -1 |
| 161 | -1 | +08:13:33.8 | -05:53:46 | 17.615 | 11.734 | 11.917 | 15.487 | 15.284 | 0.023 | 0.001 | 0.001 | 0.011 | 0.022 | 0 | 0 | 0 | 0 | 0 | -1 |
| 168 | 1129 | +08:13:24.3 | -05:44:29 | 13.243 | 12.112 | 12.010 | 12.050 | 12.100 | 0.001 | 0.001 | 0.001 | 0.001 | 0.002 | 0 | 0 | 0 | 0 | 0 | -1 |
| 172 | 1265 | +08:13:40.5 | -05:52:24 | 13.331 | 12.231 | 12.089 | 12.090 | 12.142 | 0.001 | 0.001 | 0.001 | 0.001 | 0.002 | 0 | 0 | 0 | 0 | 0 | 78 |
| 175 | 1474 | +08:14:06.5 | -05:46:02 | 13.320 | 12.209 | 12.113 | 12.158 | 12.228 | 0.001 | 0.001 | 0.001 | 0.001 | 0.002 | 0 | 0 | 0 | 0 | 0 | -1 |
| 177 | -1 | +08:13:33.6 | -05:49:39 | 13.440 | 12.370 | 12.136 | 12.106 | 12.146 | 0.002 | 0.001 | 0.001 | 0.001 | 0.002 | 0 | 0 | 0 | 0 | 0 | -1 |
| 182 | -1 | +08:13:31.8 | -05:49:29 | 13.504 | 12.459 | 12.206 | 12.163 | 12.196 | 0.002 | 0.001 | 0.001 | 0.001 | 0.002 | 0 | 0 | 0 | 0 | 0 | -1 |
| 187 | 1444 | +08:14:01.9 | -05:46:51 | 13.616 | 12.520 | 12.231 | 12.166 | 12.179 | 0.002 | 0.001 | 0.001 | 0.001 | 0.002 | 0 | 0 | 0 | 0 | 0 | 94 |

Table 4—Continued

| Star ID | WEBDA ID | RA | DEC | Magnitude | | | | | Magnitude Error | | | | | Saturation Flag | | | | | Membership Probability |
|---|---|---|---|---|---|---|---|---|---|---|---|---|---|---|---|---|---|---|---|
| | | | | $u'$ | $g'$ | $r'$ | $i'$ | $z'$ | $u'$ | $g'$ | $r'$ | $i'$ | $z'$ | $u'$ | $g'$ | $r'$ | $i'$ | $z'$ | |
| 1 | 2 | 3 | 4 | 5 | 6 | 7 | 8 | 9 | 10 | 11 | 12 | 13 | 14 | 15 | 16 | 17 | 18 | 19 | 20 |
| 194 | -1 | +08:12:58.3 | -05:45:38 | 15.218 | 13.036 | 12.290 | 12.022 | 11.882 | 0.005 | 0.001 | 0.001 | 0.001 | 0.002 | 0 | 0 | 0 | 0 | 0 | -1 |

Column (1): ID numbers are ordered in increasing r' magnitude. For multiple observations of a star the r' magnitude with smallest error is used.
Column (2): A value of -1 indicated that there was no webda entry matching the star's coordinates.
Column (3): DEC is listed in 2000 coordinates in HH:MM:SS.S format.
Column (4): DEC is listed in 2000 coordinates in DD:MM:SS format.
Columns (5-14): A value of -100.000 indicated either saturation or no detection
Columns (15-19):A saturation flag of 1 indicates either no detection or saturations.
Column (20):A membership probability of -1 indicated that there is no membership information for that star

Table 5. Example of Available Data for the Photometric Telescope

| Star ID | WEBDA ID | RA | DEC | Magnitude $u'$ | Magnitude $g'$ | Magnitude $r'$ | Magnitude $i'$ | Magnitude $z'$ | Magnitude Error $u'$ | Magnitude Error $g'$ | Magnitude Error $r'$ | Magnitude Error $i'$ | Magnitude Error $z'$ | Saturation Flag $u'$ | Saturation Flag $g'$ | Saturation Flag $r'$ | Saturation Flag $i'$ | Saturation Flag $z'$ | Membership Probability |
|---|---|---|---|---|---|---|---|---|---|---|---|---|---|---|---|---|---|---|---|
| 1 | 2 | 3 | 4 | 5 | 6 | 7 | 8 | 9 | 10 | 11 | 12 | 13 | 14 | 15 | 16 | 17 | 18 | 19 | 20 |
| 9 | 1241 | +08:13:38.0 | -06:01:32 | 12.741 | 10.062 | 9.150 | 8.819 | 8.662 | 0.006 | 0.003 | 0.004 | 0.005 | 0.001 | 0 | 0 | 0 | 0 | 0 | -1 |
| 34 | 1367 | +08:13:52.9 | -05:42:46 | 10.342 | -100.000 | 9.490 | 9.672 | 9.790 | 0.002 | -100.000 | 0.004 | 0.005 | 0.002 | 0 | 1 | 0 | 0 | 0 | 97 |
| 22 | 1616 | +08:14:26.3 | -05:44:34 | 12.886 | 10.341 | 9.493 | 9.188 | 9.042 | 0.006 | 0.003 | 0.004 | 0.005 | 0.001 | 0 | 0 | 0 | 0 | 0 | 2 |
| 29 | 1521 | +08:14:12.5 | -05:33:57 | 10.743 | 9.702 | 9.504 | 9.461 | 9.501 | 0.002 | 0.003 | 0.004 | 0.005 | 0.002 | 0 | 0 | 0 | 0 | 0 | 0 |
| 25 | 978 | +08:13:05.3 | -05:45:00 | 10.391 | 9.324 | 9.516 | 9.711 | 9.841 | 0.002 | 0.003 | 0.004 | 0.005 | 0.002 | 0 | 0 | 0 | 0 | 0 | 96 |
| 28 | 1169 | +08:13:28.6 | -05:48:15 | 10.427 | 9.382 | 9.568 | 9.761 | 9.896 | 0.002 | 0.003 | 0.004 | 0.005 | 0.002 | 0 | 0 | 0 | 0 | 0 | 96 |
| 32 | 920 | +08:12:58.5 | -05:34:08 | 10.508 | 9.394 | 9.569 | 9.752 | 9.870 | 0.002 | 0.003 | 0.004 | 0.005 | 0.002 | 0 | 0 | 0 | 0 | 0 | 92 |
| 40 | 1765 | +08:14:48.5 | -05:48:43 | 10.996 | 9.801 | 9.787 | 9.885 | 9.988 | 0.002 | 0.003 | 0.004 | 0.005 | 0.002 | 0 | 0 | 0 | 0 | 0 | 0 |
| 37 | 1183 | +08:13:30.4 | -06:04:04 | 10.901 | 9.751 | 9.798 | 9.915 | 10.022 | 0.002 | 0.003 | 0.004 | 0.005 | 0.002 | 0 | 0 | 0 | 0 | 0 | -1 |
| 38 | 1253 | +08:13:39.6 | -05:47:14 | 10.806 | 9.689 | 9.798 | 9.946 | 10.035 | 0.002 | 0.003 | 0.004 | 0.005 | 0.002 | 0 | 0 | 0 | 0 | 0 | 95 |
| 39 | 1117 | +08:13:23.1 | -05:45:23 | 10.640 | 9.622 | 9.826 | 10.030 | 10.157 | 0.002 | 0.003 | 0.004 | 0.005 | 0.002 | 0 | 0 | 0 | 0 | 0 | 97 |
| 41 | 1434 | +08:13:59.6 | -05:53:23 | 14.364 | 11.046 | 9.886 | 9.423 | 9.178 | 0.017 | 0.003 | 0.004 | 0.005 | 0.002 | 0 | 0 | 0 | 0 | 0 | 41 |
| 42 | 1600 | +08:14:24.1 | -05:31:15 | 12.483 | 10.567 | 9.912 | 9.678 | 9.604 | 0.005 | 0.003 | 0.004 | 0.005 | 0.002 | 0 | 0 | 0 | 0 | 0 | -1 |
| 45 | 1338 | +08:13:48.9 | -05:44:23 | 10.750 | 9.760 | 9.960 | 10.148 | 10.279 | 0.002 | 0.003 | 0.004 | 0.005 | 0.002 | 0 | 0 | 0 | 0 | 0 | 96 |
| 44 | 975 | +08:13:04.9 | -05:53:04 | 10.877 | 9.799 | 9.964 | 10.149 | 10.274 | 0.002 | 0.003 | 0.004 | 0.005 | 0.002 | 0 | 0 | 0 | 0 | 0 | 89 |
| 46 | 1642 | +08:14:30.7 | -05:46:53 | 11.207 | 10.113 | 9.996 | 10.005 | 10.070 | 0.002 | 0.003 | 0.004 | 0.005 | 0.002 | 0 | 0 | 0 | 0 | 0 | 0 |
| 50 | 1147 | +08:13:26.5 | -05:49:54 | 10.863 | 9.833 | 10.041 | 10.238 | 10.384 | 0.002 | 0.003 | 0.004 | 0.005 | 0.002 | 0 | 0 | 0 | 0 | 0 | 95 |
| 51 | 1281 | +08:13:43.3 | -05:41:33 | 10.840 | 9.826 | 10.043 | 10.251 | 10.378 | 0.002 | 0.003 | 0.004 | 0.005 | 0.002 | 0 | 0 | 0 | 0 | 0 | 97 |
| 56 | 1256 | +08:13:40.3 | -05:42:20 | 11.105 | 10.002 | 10.159 | 10.327 | 10.451 | 0.002 | 0.003 | 0.004 | 0.005 | 0.002 | 0 | 0 | 0 | 0 | 0 | 97 |
| 58 | 1382 | +08:13:54.3 | -05:58:47 | 11.049 | 10.023 | 10.221 | 10.418 | 10.552 | 0.002 | 0.003 | 0.004 | 0.005 | 0.002 | 0 | 0 | 0 | 0 | 0 | 96 |
| 60 | 1453 | +08:14:03.1 | -05:41:44 | 11.011 | 10.005 | 10.227 | 10.433 | 10.575 | 0.002 | 0.003 | 0.004 | 0.005 | 0.002 | 0 | 0 | 0 | 0 | 0 | 94 |
| 57 | 1529 | +08:14:13.7 | -05:27:20 | 12.326 | 10.826 | 10.248 | 10.066 | 9.976 | 0.004 | 0.003 | 0.004 | 0.005 | 0.002 | 0 | 0 | 0 | 0 | 0 | -1 |
| 61 | 1306 | +08:13:45.9 | -05:46:02 | 11.266 | 10.216 | 10.299 | 10.432 | 10.534 | 0.002 | 0.003 | 0.004 | 0.005 | 0.002 | 0 | 0 | 0 | 0 | 0 | -1 |
| 62 | 1029 | +08:13:12.1 | -05:46:42 | 11.315 | 10.229 | 10.360 | 10.515 | 10.629 | 0.003 | 0.003 | 0.004 | 0.005 | 0.002 | 0 | 0 | 0 | 0 | 0 | 96 |
| 63 | 1337 | +08:13:48.2 | -06:05:43 | 13.751 | 11.283 | 10.452 | 10.159 | 10.000 | 0.011 | 0.003 | 0.004 | 0.005 | 0.002 | 0 | 0 | 0 | 0 | 0 | 10 |
| 64 | -1 | +08:13:19.6 | -05:33:37 | 11.362 | 10.271 | 10.467 | -100.000 | 10.600 | 0.003 | 0.003 | 0.004 | -100.000 | 0.002 | 0 | 0 | 0 | 1 | 0 | -1 |
| 52 | -1 | +08:13:43.1 | -05:45:53 | 11.343 | 10.285 | 10.497 | 10.679 | 10.759 | 0.003 | 0.003 | 0.004 | 0.005 | 0.002 | 0 | 0 | 0 | 0 | 0 | -1 |
| 65 | 848 | +08:12:48.5 | -05:53:44 | 11.743 | 10.625 | 10.521 | 10.564 | 10.637 | 0.003 | 0.003 | 0.004 | 0.005 | 0.002 | 0 | 0 | 0 | 0 | 0 | 52 |
| 66 | -1 | +08:13:26.4 | -05:42:34 | 11.867 | 10.805 | 10.537 | 10.484 | 10.499 | 0.003 | 0.003 | 0.004 | 0.005 | 0.002 | 0 | 0 | 0 | 0 | 0 | -1 |
| 68 | 1069 | +08:13:17.5 | -05:41:13 | 11.449 | 10.377 | 10.558 | 10.747 | 10.877 | 0.003 | 0.003 | 0.004 | 0.005 | 0.003 | 0 | 0 | 0 | 0 | 0 | 87 |
| 69 | 1576 | +08:14:20.2 | -05:39:57 | 11.435 | 10.375 | 10.581 | 10.772 | 10.914 | 0.003 | 0.003 | 0.004 | 0.005 | 0.003 | 0 | 0 | 0 | 0 | 0 | -1 |
| 72 | 1362 | +08:13:52.0 | -05:54:20 | 11.605 | 10.496 | 10.595 | 10.734 | 10.843 | 0.003 | 0.003 | 0.004 | 0.005 | 0.003 | 0 | 0 | 0 | 0 | 0 | 91 |
| 70 | 1388 | +08:13:55.0 | -05:57:58 | 12.388 | 11.053 | 10.604 | 10.473 | 10.461 | 0.005 | 0.003 | 0.004 | 0.005 | 0.002 | 0 | 0 | 0 | 0 | 0 | -1 |
| 71 | 1449 | +08:14:02.3 | -05:56:47 | 11.545 | 10.440 | 10.604 | 10.797 | 10.966 | 0.003 | 0.003 | 0.004 | 0.005 | 0.003 | 0 | 0 | 0 | 0 | 0 | 96 |
| 76 | 1276 | +08:13:42.8 | -05:35:47 | 11.508 | 10.477 | 10.636 | 10.837 | 10.973 | 0.003 | 0.003 | 0.004 | 0.005 | 0.003 | 0 | 0 | 0 | 0 | 0 | 95 |
| 75 | 1042 | +08:13:13.7 | -05:56:38 | 11.564 | 10.488 | 10.657 | 10.836 | 10.978 | 0.003 | 0.003 | 0.004 | 0.005 | 0.003 | 0 | 0 | 0 | 0 | 0 | 88 |
| 77 | 1406 | +08:13:57.3 | -05:48:15 | 11.601 | 10.504 | 10.667 | 10.847 | 10.977 | 0.003 | 0.003 | 0.004 | 0.005 | 0.003 | 0 | 0 | 0 | 0 | 0 | 94 |
| 79 | 1424 | +08:13:58.9 | -05:50:40 | 11.834 | 10.676 | 10.719 | 10.844 | 10.952 | 0.003 | 0.003 | 0.004 | 0.005 | 0.003 | 0 | 0 | 0 | 0 | 0 | 96 |
| 83 | 1677 | +08:14:36.5 | -05:45:53 | 11.865 | 10.758 | 10.804 | 10.910 | 11.012 | 0.003 | 0.003 | 0.004 | 0.005 | 0.003 | 0 | 0 | 0 | 0 | 0 | -1 |
| 82 | 1632 | +08:14:28.0 | -06:02:46 | 11.869 | 10.731 | 10.808 | 10.941 | 11.050 | 0.003 | 0.003 | 0.004 | 0.005 | 0.003 | 0 | 0 | 0 | 0 | 0 | 18 |
| 81 | 1454 | +08:14:02.9 | -05:50:27 | 12.404 | 11.199 | 10.811 | 10.692 | 10.681 | 0.005 | 0.003 | 0.004 | 0.005 | 0.002 | 0 | 0 | 0 | 0 | 0 | 0 |
| 84 | 1214 | +08:13:34.6 | -05:55:37 | 13.963 | 11.631 | 10.830 | 10.556 | 10.414 | 0.013 | 0.004 | 0.004 | 0.005 | 0.002 | 0 | 0 | 0 | 0 | 0 | 0 |
| 87 | 1694 | +08:14:39.1 | -05:51:47 | 11.793 | 10.694 | 10.850 | 11.023 | 11.144 | 0.003 | 0.003 | 0.004 | 0.005 | 0.003 | 0 | 0 | 0 | 0 | 0 | 88 |
| 88 | 1470 | +08:14:05.3 | -05:56:32 | 11.799 | 10.714 | 10.876 | 11.050 | 11.189 | 0.003 | 0.003 | 0.004 | 0.005 | 0.003 | 0 | 0 | 0 | 0 | 0 | -1 |
| 89 | 1586 | +08:14:21.7 | -05:47:23 | 12.068 | 10.944 | 10.938 | 11.002 | 11.095 | 0.004 | 0.003 | 0.004 | 0.005 | 0.003 | 0 | 0 | 0 | 0 | 0 | 97 |
| 86 | 1230 | +08:13:36.6 | -05:51:23 | 14.833 | 11.930 | 10.943 | 10.577 | 10.498 | 0.025 | 0.004 | 0.004 | 0.005 | 0.002 | 0 | 0 | 0 | 0 | 0 | 57 |
| 96 | 1458 | +08:14:04.1 | -05:28:45 | 12.184 | 11.101 | 10.968 | 10.964 | 11.017 | 0.004 | 0.003 | 0.004 | 0.005 | 0.003 | 0 | 0 | 0 | 0 | 0 | -1 |
| 92 | 1804 | +08:14:55.2 | -05:34:45 | 13.590 | 11.632 | 10.969 | 10.739 | 10.637 | 0.010 | 0.004 | 0.004 | 0.005 | 0.002 | 0 | 0 | 0 | 0 | 0 | -1 |
| 93 | -1 | +08:13:40.9 | -05:46:57 | 12.025 | 10.897 | 10.976 | 11.108 | 11.208 | 0.004 | 0.003 | 0.004 | 0.005 | 0.003 | 0 | 0 | 0 | 0 | 0 | 87 |

Table 5—Continued

| Star ID | WEBDA ID | RA | DEC | Magnitude | | | | | Magnitude Error | | | | | Saturation Flag | | | | | Membership |
|---|---|---|---|---|---|---|---|---|---|---|---|---|---|---|---|---|---|---|---|
| | | | | $u'$ | $g'$ | $r'$ | $i'$ | $z'$ | $u'$ | $g'$ | $r'$ | $i'$ | $z'$ | $u'$ | $g'$ | $r'$ | $i'$ | $z'$ | Probability |
| 1 | 2 | 3 | 4 | 5 | 6 | 7 | 8 | 9 | 10 | 11 | 12 | 13 | 14 | 15 | 16 | 17 | 18 | 19 | 20 |
| 95 | 924 | +08:12:58.4 | -05:51:06 | 12.065 | 10.946 | 10.984 | 11.100 | 11.217 | 0.004 | 0.003 | 0.004 | 0.005 | 0.003 | 0 | 0 | 0 | 0 | 0 | 95 |

Column (1): ID numbers are ordered in increasing r' magnitude. For multiple observations of a star the r' magnitude with smallest error is used.
Column (2): A value of -1 indicated that there was no `webda` entry matching the star's coordinates.
Column (3): DEC is listed in 2000 coordinates in HH:MM:SS.S format.
Column (4): DEC is listed in 2000 coordinates in DD:MM:SS format.
Columns (5-14): A value of -100.000 indicated either saturation or no detection
Columns (15-19):A saturation flag of 1 indicates either no detection or saturations.
Column (20):A membership probability of -1 indicated that there is no membership information for that star

Table 6. Example of Available Data for the CTIO Curtis-Schmidt Telescope

| Star ID | WEBDA ID | RA | DEC | Magnitude | | | | | Magnitude Error | | | | | Saturation Flag | | | | |
|---|---|---|---|---|---|---|---|---|---|---|---|---|---|---|---|---|---|---|
| | | | | $u'$ | $g'$ | $r'$ | $i'$ | $z'$ | $u'$ | $g'$ | $r'$ | $i'$ | $z'$ | $u'$ | $g'$ | $r'$ | $i'$ | $z'$ |
| 1 | 2 | 3 | 4 | 5 | 6 | 7 | 8 | 9 | 10 | 11 | 12 | 13 | 14 | 15 | 16 | 17 | 18 | 19 |
| 1 | 1560 | +08:14:17.0 | -05:54:00 | 11.071 | 8.613 | 7.801 | 7.435 | 7.234 | 0.005 | 0.001 | 0.001 | 0.001 | 0.001 | 0 | 0 | 0 | 0 | 0 |
| 2 | 1073 | +08:13:17.9 | -05:38:26 | 9.629 | 8.536 | 8.714 | 8.884 | 8.968 | 0.002 | 0.001 | 0.001 | 0.002 | 0.003 | 0 | 0 | 0 | 0 | 0 |
| 3 | 1260 | +08:13:40.4 | -05:46:25 | 10.548 | 9.146 | 8.811 | 8.707 | 8.631 | 0.004 | 0.002 | 0.001 | 0.001 | 0.002 | 0 | 0 | 0 | 0 | 0 |
| 4 | 1296 | +08:13:44.8 | -05:48:00 | 11.166 | 9.446 | 8.915 | 8.740 | 8.653 | 0.005 | 0.002 | 0.001 | 0.002 | 0.002 | 0 | 0 | 0 | 0 | 0 |
| 5 | 776 | +08:12:37.1 | -05:40:50 | 11.690 | 9.712 | 9.022 | 8.822 | 8.711 | 0.006 | 0.002 | 0.001 | 0.002 | 0.002 | 0 | 0 | 0 | 0 | 0 |
| 6 | 1628 | +08:14:28.1 | -05:42:16 | 12.052 | 9.823 | 9.063 | 8.823 | 8.679 | 0.007 | 0.002 | 0.001 | 0.002 | 0.002 | 0 | 0 | 0 | 0 | 0 |
| 8 | -1 | +08:14:17.2 | -05:54:00 | 11.056 | 9.182 | 9.101 | 8.604 | 8.423 | 0.002 | 0.001 | 0.001 | 0.001 | 0.001 | 0 | 0 | 0 | 0 | 0 |
| 7 | 1313 | +08:13:46.6 | -05:44:52 | 10.010 | 8.918 | 9.102 | 9.267 | 9.375 | 0.003 | 0.001 | 0.001 | 0.002 | 0.003 | 0 | 0 | 0 | 0 | 0 |
| 9 | 1241 | +08:13:38.0 | -06:01:32 | 12.707 | 10.066 | 9.136 | 8.810 | 8.614 | 0.010 | 0.002 | 0.002 | 0.002 | 0.002 | 0 | 0 | 0 | 0 | 0 |
| 10 | 1832 | +08:15:00.1 | -05:32:04 | 10.894 | 9.589 | 9.182 | 9.086 | 8.995 | 0.002 | 0.002 | 0.002 | 0.001 | 0.001 | 0 | 0 | 0 | 0 | 0 |
| 12 | 870 | +08:12:51.2 | -05:50:50 | 12.449 | 10.101 | 9.242 | 8.936 | 8.750 | 0.009 | 0.002 | 0.002 | 0.002 | 0.002 | 0 | 0 | 0 | 0 | 0 |
| 14 | 1005 | +08:13:08.5 | -05:38:35 | 10.092 | 9.046 | 9.278 | 9.457 | 9.561 | 0.003 | 0.001 | 0.002 | 0.002 | 0.003 | 0 | 0 | 0 | 0 | 0 |
| 15 | 1320 | +08:13:47.6 | -05:37:25 | 9.845 | 9.275 | 9.424 | 9.229 | 9.206 | 0.001 | 0.001 | 0.001 | 0.001 | 0.001 | 0 | 0 | 0 | 0 | 0 |
| 16 | 1260 | +08:13:40.5 | -05:46:25 | 10.553 | 9.414 | 9.428 | 9.049 | 8.670 | 0.001 | 0.001 | 0.001 | 0.001 | 0.001 | 0 | 0 | 0 | 0 | 0 |
| 17 | -1 | +08:13:45.0 | -05:48:00 | 11.168 | 9.600 | 9.468 | 9.316 | 8.655 | 0.002 | 0.001 | 0.001 | 0.001 | 0.001 | 0 | 0 | 0 | 0 | 0 |
| 18 | 773 | +08:12:36.4 | -05:39:50 | 13.135 | 10.253 | 9.482 | 9.149 | 8.623 | 0.004 | 0.001 | 0.001 | 0.001 | 0.001 | 0 | 0 | 0 | 0 | 0 |
| 19 | 1541 | +08:14:15.4 | -05:43:15 | 10.120 | 9.459 | 9.490 | 9.323 | 9.366 | 0.001 | 0.001 | 0.001 | 0.001 | 0.001 | 0 | 0 | 0 | 0 | 0 |
| 20 | 1241 | +08:13:38.1 | -06:01:31 | 12.705 | 10.059 | 9.493 | 9.114 | 8.599 | 0.004 | 0.001 | 0.001 | 0.001 | 0.001 | 0 | 0 | 0 | 0 | 0 |
| 21 | -1 | +08:14:16.2 | -05:54:00 | 11.042 | 10.018 | 9.496 | 8.604 | 8.400 | 0.002 | 0.001 | 0.001 | 0.001 | 0.001 | 0 | 0 | 0 | 0 | 0 |
| 22 | 1616 | +08:14:26.3 | -05:44:34 | 12.906 | 10.358 | 9.499 | 9.206 | 9.014 | 0.011 | 0.003 | 0.002 | 0.002 | 0.003 | 0 | 0 | 0 | 0 | 0 |
| 13 | 1218 | +08:13:35.4 | -05:53:02 | 11.797 | 9.912 | 9.503 | 9.070 | 8.925 | 0.002 | 0.001 | 0.001 | 0.001 | 0.001 | 0 | 0 | 0 | 0 | 0 |
| 23 | -1 | +08:14:28.3 | -05:42:16 | 12.066 | 9.825 | 9.511 | 9.046 | 8.682 | 0.003 | 0.001 | 0.001 | 0.001 | 0.001 | 0 | 0 | 0 | 0 | 0 |
| 11 | 1289 | +08:13:44.2 | -05:48:48 | 9.991 | 9.383 | 9.513 | 9.413 | 9.521 | 0.001 | 0.001 | 0.001 | 0.001 | 0.001 | 0 | 0 | 0 | 0 | 0 |
| 24 | 1313 | +08:13:46.8 | -05:44:52 | 9.980 | 9.940 | 9.518 | 9.289 | 9.356 | 0.001 | 0.001 | 0.001 | 0.001 | 0.001 | 0 | 0 | 0 | 0 | 0 |
| 26 | -1 | +08:13:17.6 | -05:38:26 | 9.658 | 9.281 | 9.540 | 9.031 | 8.981 | 0.001 | 0.001 | 0.001 | 0.001 | 0.001 | 0 | 0 | 0 | 0 | 0 |
| 27 | -1 | +08:12:37.4 | -05:40:50 | 11.690 | 9.817 | 9.559 | 9.309 | 8.730 | 0.002 | 0.001 | 0.001 | 0.001 | 0.001 | 0 | 0 | 0 | 0 | 0 |
| 29 | 1521 | +08:14:12.5 | -05:33:57 | 10.768 | 9.729 | 9.639 | 9.491 | 9.498 | 0.001 | 0.001 | 0.001 | 0.001 | 0.003 | 0 | 0 | 0 | 0 | 0 |
| 30 | 870 | +08:12:51.4 | -05:50:50 | 12.469 | 10.118 | 9.642 | 9.055 | 8.775 | 0.003 | 0.001 | 0.001 | 0.001 | 0.001 | 0 | 0 | 0 | 0 | 0 |
| 31 | 1616 | +08:14:26.5 | -05:44:34 | 12.886 | 10.359 | 9.675 | 9.264 | 9.013 | 0.004 | 0.001 | 0.001 | 0.001 | 0.001 | 0 | 0 | 0 | 0 | 0 |
| 32 | 920 | +08:12:58.5 | -05:34:08 | 10.526 | 9.562 | 9.676 | 9.797 | 9.888 | 0.001 | 0.001 | 0.001 | 0.001 | 0.002 | 0 | 0 | 0 | 0 | 0 |
| 28 | 1169 | +08:13:28.6 | -05:48:15 | 10.425 | 9.604 | 9.678 | 9.774 | 9.888 | 0.001 | 0.001 | 0.001 | 0.001 | 0.002 | 0 | 0 | 0 | 0 | 0 |
| 33 | -1 | +08:13:08.7 | -05:38:35 | 10.102 | 9.703 | 9.679 | 9.482 | 9.566 | 0.001 | 0.001 | 0.001 | 0.001 | 0.001 | 0 | 0 | 0 | 0 | 0 |
| 34 | 1367 | +08:13:52.9 | -05:42:46 | 10.341 | 9.482 | 9.727 | 9.696 | 9.804 | 0.001 | 0.001 | 0.001 | 0.001 | 0.002 | 0 | 0 | 0 | 0 | 0 |
| 25 | 978 | +08:13:05.3 | -05:45:00 | 10.401 | 9.577 | 9.746 | 9.736 | 9.823 | 0.001 | 0.001 | 0.001 | 0.001 | 0.002 | 0 | 0 | 0 | 0 | 0 |
| 35 | -1 | +08:12:36.7 | -05:40:50 | 11.690 | 9.820 | 9.756 | 9.309 | 8.730 | 0.002 | 0.001 | 0.001 | 0.001 | 0.001 | 0 | 0 | 0 | 0 | 0 |
| 36 | -1 | +08:13:18.6 | -05:38:26 | 9.645 | 10.048 | 9.763 | -100.000 | 8.973 | 0.001 | 0.001 | 0.001 | -100.000 | 0.001 | 0 | 0 | 0 | 1 | 0 |
| 38 | 1183 | +08:13:30.4 | -06:04:04 | 10.889 | 9.769 | 9.810 | 9.900 | 9.963 | 0.002 | 0.001 | 0.001 | 0.001 | 0.002 | 0 | 0 | 0 | 0 | 0 |
| 40 | 1765 | +08:14:48.5 | -05:48:43 | 11.009 | 9.808 | 9.839 | 9.890 | 9.965 | 0.002 | 0.001 | 0.001 | 0.001 | 0.002 | 0 | 0 | 0 | 0 | 0 |
| 37 | 1253 | +08:13:39.6 | -05:47:14 | 10.796 | 9.699 | 9.881 | 9.970 | 10.042 | 0.001 | 0.001 | 0.001 | 0.001 | 0.002 | 0 | 0 | 0 | 0 | 0 |
| 41 | 1434 | +08:13:59.6 | -05:53:22 | 14.351 | 11.063 | 9.883 | 9.420 | 9.148 | 0.008 | 0.002 | 0.001 | 0.001 | 0.001 | 0 | 0 | 0 | 0 | 0 |
| 39 | 1117 | +08:13:23.0 | -05:45:23 | -100.000 | 9.708 | 9.885 | -100.000 | -100.000 | -100.000 | 0.001 | 0.001 | -100.000 | -100.000 | 1 | 0 | 0 | 1 | 1 |
| 42 | 1600 | +08:14:24.1 | -05:31:15 | 12.515 | 10.583 | 9.913 | 9.697 | 9.590 | 0.003 | 0.001 | 0.001 | 0.001 | 0.001 | 0 | 0 | 0 | 0 | 0 |
| 43 | 1726 | +08:14:43.2 | -05:27:07 | 10.783 | 9.725 | 9.941 | 10.110 | 10.214 | 0.001 | 0.001 | 0.001 | 0.001 | 0.002 | 0 | 0 | 0 | 0 | 0 |
| 45 | 1338 | +08:13:48.9 | -05:44:23 | 10.775 | 9.795 | 9.992 | 10.172 | 10.278 | 0.001 | 0.001 | 0.001 | 0.001 | 0.002 | 0 | 0 | 0 | 0 | 0 |
| 46 | 1642 | +08:14:30.7 | -05:46:53 | 11.209 | 10.111 | 9.995 | 10.006 | 10.028 | 0.002 | 0.001 | 0.001 | 0.001 | 0.002 | 0 | 0 | 0 | 0 | 0 |
| 44 | 975 | +08:13:04.9 | -05:53:04 | 10.883 | 9.818 | 10.011 | 10.177 | 10.252 | 0.002 | 0.001 | 0.001 | 0.001 | 0.002 | 0 | 0 | 0 | 0 | 0 |
| 47 | -1 | +08:14:14.7 | -05:54:01 | -100.000 | -100.000 | 10.027 | 9.878 | -100.000 | -100.000 | -100.000 | 0.001 | 0.001 | -100.000 | 1 | 1 | 0 | 0 | 1 |
| 48 | 1527 | +08:14:12.0 | -06:09:08 | 10.981 | 9.879 | 10.037 | 10.174 | 10.291 | 0.002 | 0.001 | 0.001 | 0.001 | 0.002 | 0 | 0 | 0 | 0 | 0 |
| 50 | 1147 | +08:13:26.5 | -05:49:53 | 10.869 | 9.846 | 10.067 | 10.261 | 10.369 | 0.002 | 0.001 | 0.001 | 0.001 | 0.002 | 0 | 0 | 0 | 0 | 0 |

Table 6—Continued

| Star ID | WEBDA ID | RA | DEC | Magnitude | | | | | Magnitude Error | | | | | Saturation Flag | | | | | Membership Probability |
|---|---|---|---|---|---|---|---|---|---|---|---|---|---|---|---|---|---|---|---|
| | | | | $u'$ | $g'$ | $r'$ | $i'$ | $z'$ | $u'$ | $g'$ | $r'$ | $i'$ | $z'$ | $u'$ | $g'$ | $r'$ | $i'$ | $z'$ | |
| 1 | 2 | 3 | 4 | 5 | 6 | 7 | 8 | 9 | 10 | 11 | 12 | 13 | 14 | 15 | 16 | 17 | 18 | 19 | 20 |
| 52 | 1281 | +08:13:43.3 | -05:41:33 | 10.857 | 9.837 | 10.077 | 10.265 | 10.383 | 0.002 | 0.001 | 0.001 | 0.001 | 0.002 | 0 | 0 | 0 | 0 | 0 | 97 |

Column (1): ID numbers are ordered in increasing r' magnitude. For multiple observations of a star the r' magnitude with smallest error is used.
Column (2): A value of -1 indicated that there was no `webda` entry matching the star's coordinates.
Column (3): DEC is listed in 2000 coordinates in HH:MM:SS.S format.
Column (4): DEC is listed in 2000 coordinates in DD:MM:SS format.
Columns (5-14): A value of -100.000 indicated either saturation or no detection
Columns (15-19):A saturation flag of 1 indicates either no detection or saturations.
Column (20):A membership probability of -1 indicated that there is no membership information for that star